Title

Contribution of NK cells to immunotherapy mediated by PD-1/PD-L1 blockade.

Journal

The Journal of clinical investigation, 128(10)

ISSN

0021-9738

Authors

Hsu, Joy
Hodgins, Jonathan J
Marathe, Malvika
et al.

Publication Date

2018-10-01

DOI

10.1172/jci99317

Peer reviewed

Title page:

Contribution of NK cells to immunotherapy mediated by PD-1/PD-L1 blockade.

Joy Hsu[1,†], Jonathan J. Hodgins[2,3,†], Malvika Marathe[1], Chris J. Nicolai[1], Marie-Claude Bourgeois-Daigneault[2,3], Troy N. Trevino[1], Camillia S. Azimi[1], Amit K. Scheer[2,3], Haley E. Randolph[1], Thornton W. Thompson[1], Lily Zhang[1], Alexandre Iannello[1], Nikhita Mathur[2,3], Karen E. Jardine[2,3], Georgia A. Kirn[1], John C. Bell[2,3], Michael W. McBurney[2,3], David H. Raulet[1,*] Michele Ardolino[1,2,3,*]

1: Department of Molecular and Cell Biology, Immunotherapy and Vaccine Research Initiative, Cancer Research Laboratory, Division of Immunology and Pathogenesis, University of California, Berkeley, Berkeley, CA, 94720, USA.

2: Department of Biochemistry, Microbiology and Immunology, University of Ottawa, Ottawa, ON K1H 8M5, Canada

3: Centre for Cancer Therapeutics, Ottawa Hospital Research Institute, Ottawa, ON K1H 8L6, Canada

†: JH and JJH equally contributed to this study.

*: DHR and MA equally contributed to this study.

correspondence to:

raulet@berkeley.edu

tel: 510-642-9521

485 LSA, Berkeley, CA, 94720-3200

and

m.ardolino@uottawa.ca

tel: 613-737-8899 x 77257

501 Smyth Road, Cancer Center, 3-328, Ottawa, ON, K1H8M2

Conflict of interest statement:

DHR is a co-founder of Dragonfly Therapeutics, and served on the Scientific Advisory Boards of Innate Pharma, Aduro Biotech and Ignite Immmunotherapy; he has a financial interest in all four companies and received research support from Innate Pharma. JCB is a co-founder and have equity in Turnstone Biologics from whom he receives a consulting fees and research support for his lab. MCBD and JCB have both patented intellectual properties, not related to the present article.

Abstract:

Checkpoint blockade immunotherapy targeting the PD-1/PD-L1 inhibitory axis has produced remarkable results in the treatment of several types of cancer. Whereas cytotoxic T cells are known to provide important anti-tumor effects during checkpoint blockade, certain cancers with low MHC expression are responsive to therapy, suggesting that other immune cell types may also play a role. Here, we employed several mouse models of cancer to investigate the effect of PD-1/PD-L1 blockade on natural killer (NK) cells, a population of cytotoxic innate lymphocytes that also mediate anti-tumor immunity. We discovered that PD-1 and PD-L1 blockade elicited a strong NK cell response that was indispensable for the therapeutic effect of immunotherapy. PD-1 was expressed on NK cells within transplantable, spontaneous and genetically-induced mouse tumor models and PD-L1 expression in cancer cells resulted in reduced NK cell responses and generation of more aggressive tumors in vivo. PD-1 expression was more abundant on NK cells with an activated and more responsive phenotype and did not mark NK cells with an exhausted phenotype. These results demonstrate the importance of the PD-1/PD-L1 axis in inhibiting NK cell responses in vivo and reveal that NK cells, in addition to T cells, mediate the effect of PD-1/PD-L1 blockade immunotherapy.

Main text

Introduction

Immunotherapy targeting the PD-1/PD-L1 inhibitory axis has produced spectacular results in the treatment of a wide variety of tumors (1-9). The current paradigm dictates that CD8 T cells are inhibited by PD-1 and it is widely accepted that checkpoint blockade unleashes T cells to attack tumor cells. However, many cancer types exhibit a high incidence of MHC loss and/or low neoantigen burden (10, 11), which should render tumor cells refractory to recognition by CD8 T

cells. High levels of PD-L1 expression have been observed in tumors with low MHC I expression (12-18). Interestingly, some of these cancer types are responsive to PD-1/PD-L1 blockade. An example is Hodgkin's Lymphoma (12, 13), in which genes encoding PD-L1 are amplified. Interestingly, in Hodgkin's Lymphoma, PD-L1 upregulation was predictive of a poor outcome even when the tumor cells were defective in MHC I expression (19). These findings suggested the existence of immune responses that are independent of cytotoxic T cells, inhibited by PD-1 and rescued by PD-1-blockade.

NK cells are innate lymphocytes with cytotoxic activity against cancer cells that also orchestrate the immune response by releasing cytokines and chemokines (20). NK cells participate in the immune response against solid and hematopoietic cancers owing to their capacity to recognize molecular patterns characteristic of stressed cells (so-called *missing-self* and *induced-self* recognition (21)). NK cells mediate strong anti-leukemia activity when included in some allogeneic stem cell transplants (22-31) and their presence in solid tumors is a good prognostic factor (31-37). Unlike recognition by T cells, recognition by NK cells does not require that cancer cells express neoantigens or over-express self-antigens, and loss of MHC expression on tumor cells increases rather than decreases their susceptibility to NK cell killing (38, 39). Evidence that PD-1 can be expressed on human NK cells has recently emerged in several cancer indications, including Hodgkin's Lymphoma (40-44), but mechanistic in vivo studies examining whether and how PD-1 inhibits NK cell responses to tumors, and whether PD-1/PD-L1 blockade mobilizes NK cell responses, are still lacking.

Here, we investigated if the therapeutic effect of PD-1 and PD-L1 blockade relies on the anti-tumor activity of NK cells. Using several cancer mouse models, we found that activated NK cells express PD-1 and that PD-1 engagement by PD-L1^{+} tumor cells potently suppresses NK cell-mediated immunity to tumors. Releasing PD-1-imposed inhibition through blockade of PD-1 or PD-L1 activated an NK response that was indispensable for the full effect of PD-1/PD-L1 blockade.

Results

NK cells participate in the therapeutic effect of PD-1/PD-L1 blockade:

To study the effect of PD-1 blockade in a model where T cells do not participate in the immune response against cancer, we took advantage of a lymphoma model based on injection of RMA-S cells, which exhibit low expression of MHC I. Tumor surveillance of RMA-S cells is strongly dependent on NK cells but not T cells (45), as confirmed by experiments where depletion of NK cells, but not T cells, resulted in accelerated tumor growth (Figure 1A). RMA-S cells expresses low levels of the PD-1 ligands PD-L1 and PD-L2, even after IFN-γ treatment in vitro (Figure 1B). Even as established tumors in syngeneic mice, as tested in ex vivo tumor dissociates, expression of PD-L1 by RMA-S cells was much lower than observed on myeloid cells in the spleen or on other tumor cells such as the prostate adenocarcinoma line TRAMP-C2 (Figure 1C). We transduced RMA-S cells with *Pdl1* and selected by flow cytometry cells with surface PD-L1 at levels comparable to those observed on myeloid cells in the spleen or infiltrating the tumor, or to those naturally expressed by a PD-L1$^+$ tumor cell line in vivo (TRAMP-C2 cells, Figure 1B-C). Immunosurveillance of RMA-S-*Pdl1* tumors was not mediated by T cells, but NK-depletion accelerated the growth of tumor cells in vivo, showing that NK cells, but not T cells, mediate an immune response to this cell line even when PD-L1 is expressed (Figure 1D). Therefore, this represents a valuable model to study the effect of PD-1 blockade in a system where a CD8 T cell response to cancer cells is incapacitated by low MHC expression, but an NK cell response is still evident.

To investigate whether PD-1/PD-L1 blockade elicits an effective response for tumors that are insensitive to CD8 T cells, we injected RMA-S-*Pdl1* cells into B6 mice and after two days treated the mice with a PD-1 blocking antibody (clone RMP1-14) (46). Mice treated just once exhibited a markedly diminished rate of tumor progression (Figure 1E). However, when mice were depleted of NK cells before tumor injection, the antibody treatment was completely ineffective

(Figure 1E), showing that PD-1 blockade mobilized an NK cell response. Next, we allowed the RMA-S-*Pdl1* tumors to progress to a volume of ~25 mm^3 before initiating treatment. Even in this scenario, anti-PD-1 therapy significantly delayed tumor development (Figure 1F).

Compared to systemic injections, local injections of anti-PD-1 allow the use of a lower antibody dose while potentially reducing systemic side effects. To address the efficacy of intratumoral injection of therapeutic antibodies, RMA-S-*Pdl1* cells were mixed in Matrigel with control Ig, PD-1 antibody (a dose more than 10-fold lower than in the systemic injection) or PD-L1 antibodies, and injected subcutaneously in B6 mice. Mice that received PD-1 or PD-L1 antibody in the tumor inoculum developed significantly smaller tumors (Figure 1G-H), consistent with the results obtained by injecting the antibody i.p.. Collectively, these data show that the efficacy of PD-1 and PD-L1 blockade in MHC-deficient tumors depends on NK cell activity.

PD-1 is expressed by and inhibits NK cells:

Having shown that the efficacy of PD-1 and PD-L1 blockade depends on NK cells in a scenario where tumor cells are MHC-deficient, we determined whether PD-1 was expressed by and inhibited NK cells. We injected RMA-S cells in syngeneic mice and analyzed PD-1 expression by flow cytometry. PD-1 was strongly upregulated on 30-40% of NK cells infiltrating RMA-S tumors, but not in splenic NK cells (Figure 2A-B). PD-1 expression on intratumoral NK cells was evident at the earliest time point that allowed dissection and analysis of the cells (day 7, when tumors were small, <25 mm^3). NK cells in the local lymph nodes draining the tumor, and in some cases distant lymph nodes, showed slight PD-1 expression at early time points and higher expression later (Figure 2A and not shown). Similar results were obtained when we analyzed NK cells infiltrating tumors derived from the RMA tumor line, which is an MHC I^+ version of RMA-S cells (Figure 2C). Hence, PD-1 expression by NK cells within tumors is not limited to MHC-deficient tumors.

Next, we employed another well-established tumor model based on s.c. injection of the colon carcinoma cell line CT26 in syngeneic BALB/cJ mice. Up to 60% of NK cells infiltrating CT26 tumors expressed PD-1, whereas only modest PD-1 expression was observed on NK cells from the draining lymph nodes, and no PD-1 expression was detected on splenic NK cells (Figure 2A-C). PD-1 upregulation on NK cells was observed in numerous other tumor models including several ectopic s.c. models and three spontaneous models (Figure 2C). Interestingly, we found that PD-1 was expressed with a high degree of heterogeneity among tumor bearing mice both in NK and CD8+ T cells (Figure 2C).

To study the functional effects of PD-1 engagement on NK cells, we initially used an in vitro approach. Compared to untransduced tumor cells, tumor cells transduced with PD-L1 were less effective in inducing degranulation and IFN-γ production by PD-1$^+$ NK cells in vitro, consistent with inhibition of NK activation by PD-L1 (Figure 2D-E). The prototypical NK-sensitive human target cell line K562 lacks PD-L1 and PD-L2, and the human NK cell line NK92 lacks PD-1. Cytolysis of K562 cells by NK92 cells, and K562-induced degranulation of NK92 cells, were significantly reduced when K562 and NK92 were transduced with PD-L1 and PD-1, respectively (Figure 1E, F). Responses were minimally or not affected with empty vector-transduced NK92 cells, or when NK92-*Pdcd1* (*Pdcd1* encodes PD-1) cells were stimulated with untransduced K562 cells, demonstrating that inhibition required both receptor expression by NK cells and ligand expression by target cells.

In conclusion, PD-1 is specifically upregulated by a population of NK cells in the tumor microenvironment, and it suppresses NK cell degranulation and cytotoxic functions in vitro.

PD-1 inhibits both NK- and T cell-mediated anti-tumor immunity:

We investigated if PD-1 suppresses NK anti-tumor activity in vivo. In mice implanted with 10^6 tumor cells, RMA-S-*Pdl1* were much more aggressive than RMA-S cells (untransduced or

transduced with an empty vector) (Figure 3A). RMA-S-*Pdl1* caused fatality in ~90% of recipients, whereas only ~45% of mice injected with RMA-S cells developed fatal tumors (Figure 3B). NK-depletion before tumor cell implantation (Figure 3B, C), or genetic depletion of NK cells in *Rag1*$^{-/-}$ *Il2rg*$^{-/-}$ immuno-deficient mice (Figure 3D), resulted in similar growth of RMA-S and RMA-S-*Pdl1* tumors and similar rapid mortality, whereas depletion of CD4 and CD8 T cells had no effect (Figure 1A, D). These data verify the expectation that NK cells but not T cells mediate spontaneous rejection of RMA-S cells, and indicate that in this model NK cells are inhibited by PD-1/PD-L1 interactions and rescued by PD-1/PD-L1 blockade. The finding that NK-depletion accelerated tumor growth somewhat more potently than PD-L1 transduction of the RMA-S cells (Figure 3B, C) suggests that while PD-L1 expression by RMA-S cells strongly inhibited NK cells, some residual NK-mediated rejection still occurred.

RMA cells, unlike RMA-S, are resistant to NK cells, and also fail to provoke T cell-mediated responses when inoculated in naïve mice (45, 47). Not surprisingly, RMA tumors grew rapidly in B6 mice whether or not the tumor cells expressed PD-L1 (Figure 3E), demonstrating that PD-L1 protein expression by the tumor cells does not promote in vivo growth of tumors that are refractory to NK- (and T cell-) mediated control.

Like RMA-S, the melanoma cell line B16-BL6 (hereafter abbreviated B16) is poorly immunogenic for T cells but is sensitive to NK cells (48). We generated PD-L1-transductants of B16 (hereafter abbreviated B16-*Pdl1*). NK cells infiltrating subcutaneous B16 tumors expressed PD-1 in only half of tumor-bearing animals, and at a low frequency (Figure 2C), so it was not surprising that B16-*Pdl1* cells grew at a similar rate in vivo as the parental cells when transferred subcutaneously. In contrast, NK cells infiltrating lung tissue where B16 cells had colonized after i.v. injection had appreciable, albeit variable, PD-1 expression (Figure 4B). Compared to the parental cell line, B16-*Pdl1* cells injected i.v. caused a more rapid disease, indicating that PD-L1 expression inhibited tumor rejection (Figure 4C, E). Similar results were obtained with inocula of 5,000 or

20,000 tumor cells. With both doses, NK cell depletion accelerated the onset of lethal disease with untransduced tumor cells to match the pace of disease with PD-L1-transduced tumor cells (Figure 4C-F). In contrast, CD8 depletion did not accelerate mortality in mice injected with B16 or B16-*Pdl1* tumor cells (Sup. Figure 1). These data confirmed that B16 cells are controlled by NK cells and not CD8 T cells (i.e. in the absence of immunotherapy), and indicated that higher PD-L1 expressed by these tumor cells inhibits the NK cell response. Post-mortem analysis confirmed the higher degree of tumor burden conferred by PD-L1 expression. Twenty-one days after injecting the lower dose of tumor cells, only half of the mice that received B16 cells had macroscopically visible tumor colonies in the lungs, whereas 12 out of 13 mice injected with B16-*Pdl1* cells had easily observable lung tumors (Figure 4G). qRT-PCR analysis of lung tissue RNA for transcripts encoding a melanocyte-specific protein (*Gp100(49)*) confirmed the increased burden of B16-*Pdl1* tumors as compared to B16 cells (Figure 4H). We also attempted to address whether PD-1 blockade provided a therapeutic effect in the B16 experimental metastasis model, but were stymied in the effort by the failure of the PD-1 blocking antibody to efficiently penetrate the lung tumor microenvironment, as indicated by the absence of antibody bound to PD-1^{+} cells in dissociated tumors after treatment. Collectively, these findings indicated that PD-L1 expression inhibits NK-mediated control of B16 lung colonization.

We investigated whether PD-1-mediated inhibition of NK cell responses was physiologically relevant when T cells participated in anti-tumor immunity. Initially, we employed a tumor model based on s.c. injection of CT26 cells in BALB/cJ mice. CT26 cells express high levels of ligands for NK cell-activating receptors (Supplementary Figure 2) and are efficiently killed by IL-2-activated NK cells in vitro (not shown). CT26 cells naturally express low amounts of PD-L1 in vitro, which is strongly upregulated by IFN-γ (Figure 5A). To address the role of PD-1 inhibition in this tumor model, we generated a PD-L1-deficient variant of CT26 by targeting the *Pdl1* gene with CRISPR/Cas9. The mutation abolished PD-L1 expression whether or not the cells were treated

with IFN-γ (Figure 5A). When injected in BALB/cJ mice, CT26 cells generated solid tumors in all recipients 5-7 days after injection, whereas growth of PD-L1-KO CT26 cells was dramatically delayed, indicating that naturally expressed PD-L1 strongly inhibited the anti-tumor response (Figure 5B). In this cancer model, PD-1 was upregulated on a large fraction of both NK and T cells infiltrating the tumors (Figure 2C). To determine which immune cells were susceptible to PD-1-mediated inhibition, groups of mice were depleted of NK cells, CD8 T cells, or both, before being challenged with tumor cells. Notably, NK- or CD8-depletion resulted in substantial and similar increases in the growth rates of CT26-*Pdl1-/-* tumors, showing that PD-1 comparably inhibited NK and CD8 T cells (Figure 5B). Furthermore, depletion of both NK and CD8 T cells resulted in even faster tumor growth, comparable to the growth of wildtype CT26 cells, showing that NK cells and CD8 T cells were the major tumor-rejecting populations, that they acted at least partly independently, and that they were both inhibited by PD-L1 (Figure 5B). In contrast, with CT26 cells, depletion of NK and/or CD8 T cells had only a marginal effect on tumor growth (Figure 5C), providing additional evidence that PD-L1 expressed by CT26 strongly inhibits both NK- and CD8-mediated anti-tumor immunity.

As a control to show that the rejection of CT26-*Pdl1-/-* cells was not due to off-target effects incurred in preparing the mutants, or to the impact of the vector in the cells, we generated CT26-*Pdl1-/-* cells restored with PD-L1. PD-L1-transduced CT26-*Pdl1-/-* cells expressed PD-L1 similarly to WT cells treated with IFN-γ (Figure 5A), and grew as aggressively in vivo as wildtype CT26 cells, whereas empty vector-transduced CT26-*Pdl1-/-* cells were strongly rejected (Figure 5D). Together, these data provide compelling evidence that the rejection of CT26-*Pdl1-/-* cells was due to the PD-L1 deficiency and not to other alterations in the cells.

As PD-1 restoration inhibited NK cells in the CT26-*Pdl1-/-* model, we hypothesized that in mice with CT26 tumors that express PD-L1, PD-1 blockade would reinvigorate an NK response

that would result in better tumor rejection. The increased tumor growth resulting from restoration of PD-L1 expression in CT26-*Pdl1*$^{-/-}$ cells (Figure 5D) was reversed when the animals were injected with PD-L1 antibody (Figure 6A), indicating a therapeutic effect of PD-L1 blockade. The therapeutic impact of PD-L1 blockade was impeded when NK cells were depleted in tumor-bearing mice with two different treatment regimens (Figure 6B-C), showing that NK cells, in addition to CD8 T cells, contribute to the therapeutic effect of PD-L1 blockade.

To further corroborate these results, we employed a competitive in vivo killing assay. We injected a 1:1 mixture of PD-L1-overexpressing and PD-L1-deficient CT26 cells in mice that were depleted or not of NK cells. As shown in Figure 6D, the growth advantage of PD-L1-expressing tumor cells observed in undepleted mice was lost when mice were depleted of NK cells, indicating that NK cells preferentially kill tumor cells lacking PD-L1 expression.

Consistently, when CT26 tumors expressed PD-L1 the percentages of PD-1+ NK cells that expressed the effector molecule granzyme B intracellularly were reduced as compared to PD-1+ NK cells in PD-L1-deficient CT26 tumors, or to PD-1- NK cells (Figure 6E). These data are consistent with inhibition of NK effector function by PD-1-PD-L1 interactions in vivo. Moreover, PD-L1 antibody treatment of mice bearing CT26 tumor cells resulted in a significant increase in the percentage of granzyme B+ NK cells among PD-1+ NK cells, consistent with the impact of PD-L1 blockade on tumor rejection in vivo (Figure 6E). Several other parameters of NK cell activation were unchanged, consistent with our observation that most NK activation markers are not strongly induced by exposure to NK sensitive (as opposed to NK-resistant) tumors in vivo (MA and DHR, unpublished observations). As CT26 cells are known to express high levels of MHC I molecules and to express mutated neo-antigens (50), it was not surprising to observe such a strong T cell response with the PD-L1-deficient variants. It is, however, remarkable that in such a scenario NK cells play a comparable role to T cells and that with wildtype CT26 cells, PD-1 can potently suppress both responses.

As a fourth model, we employed orthotopic injections of 4T1 cells in the mammary fat pad of BALB/cJ mice. Similarly to CT26 cells, 4T1 cells express NK cell-activating ligands and are efficiently killed by IL-2-activated NK cells in vitro (Supplementary Figure 2 and data not shown). We generated a PD-L1-deficient version of 4T1 cells (4T1-*Pdl1*$^{-/-}$) with CRISPR/Cas9 (Figure 7A). When injected in BALB/cJ mice, 4T1 cells grew more rapidly than their PD-L1-deficient counterpart, indicating that even in this model PD-L1 expression on tumor cells suppressed the immune response (Figure 7B and D). As we observed with CT26-derived tumors, depletion of NK or CD8 T cells separately did not completely rescue the growth of PD-L1-deficient tumor cells, but concurrent depletion of NK and CD8 T cells accelerated the growth of 4T1-*Pdl1*$^{-/-}$ cells to the level observed with 4T1 cells, indicating that PD-L1 inhibition was exerted on both NK and CD8 T cells (Figure 4B-E). Therefore, in two cancer models where CD8 T cells played a significant role, NK responses were still important for controlling cancer development and PD-1 was able to suppress the anti-tumor activity of NK cells.

These results in four different tumor models show that NK-mediated anti-tumor responses are inhibited by PD-1, indicating that PD-1 represents an important checkpoint for NK cells.

PD-1 is more abundantly expressed in activated NK cells with higher functional activity:

NK cells are both phenotypically and functionally heterogeneous (20). In the analyzed tumor models, PD-1 was expressed by a discrete fraction cells rather than by the entire population. We addressed whether the NK cells that upregulated PD-1 correspond to a phenotypically defined subset. Of the four maturation stages defined by CD27 and CD11b expression (51), PD-1 was expressed on NK cells within all 4 stages, with somewhat higher expression on R2 cells ($CD11b^{+}CD27^{+}$ NK cells), one of the stages of maturation where NK cells are more responsive (Figure 8A).

Another element of heterogeneity among NK cells is provided by stochastic expression of MHC-specific inhibitory receptors (20). In B6 mice, Ly49C, Ly49I and NKG2A recognize self MHC I, whereas Ly49A and Ly49G2 do not (38). NK cells that expressed inhibitory receptors specific for the host's MHC I molecules were marginally but significantly more likely to express PD-1. This was evident when examining NK cells that simultaneously expressed all three of the known self MHC-specific receptors (Ly49C$^+$, Ly49I$^+$, and NKG2A$^+$) in B6 mice, or the larger population that expressed at least one of the three (Figure 8B). Interestingly, NK cells expressing self MHC-specific receptors exhibit greater functional responsiveness than other NK cells (38).

The more robust expression of PD-1 in NK cells with a phenotype associated with higher responsiveness led us to hypothesize that cellular activation could be related to PD-1 expression. Consistent with our hypothesis, NK cells that express activation markers like Sca-1 and CD69 consistently contained more PD-1$^+$ NK cells than NK cells lacking these markers (Figure 8C-E). Induction of PD-1 on NK cells did not, however, necessarily correlate with how well the tumor cells stimulate NK cells. Indeed, PD-1 expression was similar on NK cells infiltrating RMA-S tumors (a good NK cell target) and RMA tumors (an NK-resistant, MHC I-high sister cell line) (Figure 2C). Moreover, compared to NK-insensitive RMA tumor cells, RMA cells that were rendered NK-sensitive by transduction of the NK-activating ligands m157 or RAE-1ε (which bind the Ly49H and NKG2D activating receptors, respectively) induced only marginal increases in the percentage of PD-1 expressing NK cells (Supplementary Figure 3). The lack of a strong association between tumor cell stimulation of NK cells and PD-1 expression suggests that PD-1 upregulation may be induced more potently by other types of signals, such as local exposure to generic activating or co-activating ligands or cytokines.

The clear correlation between cellular activation markers and PD-1 expression prompted us to investigate whether PD-1$^+$ NK cells corresponded to the more functionally active NK cells. To answer this question, we took advantage of an ex vivo approach, often used to assay NK cell

responsiveness (47, 52-54). We injected RMA-S or RMA-S-*Pdl1* tumor cells in syngeneic B6 mice and, after tumor formation re-stimulated tumor-infiltrating NK cells ex vivo with plate-bound antibodies that crosslink NK cell activating receptors NKp46 or NKR-P1C, or isotype control antibodies. Degranulation (CD107a on the cell surface) and intracellular accumulation of IFN-γ were assessed. Interestingly, PD-1$^+$ NK cells had substantially higher functional activity than PD-1-negative NK cells (Figure 9). A similar result was obtained employing NK cells infiltrating PD-L1+ or PD-L1- CT26 tumors (Figure 10). These results showed that PD-1 is selectively upregulated on the most activated and functionally responsive intratumoral NK cells. These findings explain why the NK response is potently suppressed by PD-1 interactions when PD-1 is only expressed by a fraction of NK cells: the PD-1+ NK cells are the ones with the greatest potential activity and are responsible for most of the response when PD-1 interactions are blocked.

In conclusion, our studies show that PD-1/PD-L1 blockade relies on NK cells in both MHC+ and MHC- tumors. PD-1 inhibits NK-dependent immune surveillance and favors the escape of tumor cells from NK cell responses.

Discussion:

The efficacy of PD-1 blockade has been correlated with reinvigoration of a pre-existing T cell response (55). Indeed, tumors with abundant neoantigens due to an elevated mutational load, such as melanomas and lung cancers, tend to be more responsive to PD-1 blockade than tumors with a low somatic mutation load (56-59). However, the prevalent view that T cells are the only important mediators of the anti-tumor response unleashed by PD-1 blockade is challenged by at least two observations: *i)* human tumors often lose expression of HLA-I molecules (10, 60), and in some of these tumors PD-1 blockade is still effective; *ii)* a strong clinical response to PD-1 blockade is observed in tumor indications, such as Hodgkin's lymphomas, that display extremely low mutational loads (12, 13). Unlike T cells, NK cells can respond to MHC-deficient tumors (45)

and they are activated by ligands that are usually upregulated upon oncogenic stress (39, 61). Based on these premises, we hypothesized that PD-1 blockade may activate an NK cell response.

Tumors that are good T cell targets, such as melanoma and lung cancer cells, also express high levels of ligands for NK-activating receptors (62-65). Furthermore, NK cells often infiltrate melanoma and lung tumors. Hence, NK cells may also participate in immune-mediated rejection of these tumors, even if T cells may play a major role under these conditions.

Here, we present the first mechanistic evidence that PD-1 blockade elicits an anti-tumor NK cell response and that PD-1 is an important checkpoint for NK activation. We propose that along with T cells, NK cells also participate in the clinical benefit of PD-1/PD-L1 antibody therapy. NK cells may participate by helping to recruit a T cell response and/or by killing tumor cells directly. The participation of T cells vs NK cells in direct tumor killing will likely depend on the relative sensitivity of the specific tumor to NK versus T cells, which in turn varies depending on numerous factors including expression of MHC I and activating ligands for NK cells, the antigenic load of the tumor cells, PD-L1 expression by the tumor cells, and PD-1 expression by NK cells and T cells in the tumor bed. Our studies in mice, for example, show that PD-1 blockade elicits anti-tumor responses by both T cells and NK cells in the case of CT26 tumors, whereas it elicits an NK cell response in the case of RMA-S-*Pdl1* tumors, which are defective for MHC I expression. Interestingly, ~79% of classical Hodgkin's lymphomas show decreased or absent expression of MHC I (19), yet a large majority of patients respond to PD-1 blockade immunotherapy (12). These observations suggest the possibility that NK cells participate in tumor elimination stimulated by PD-1 immunotherapy in this indication and probably others. Other immune cell types such as tumor-associated macrophages, may also express PD-1 and may also play a role in therapeutic responses (66). Interestingly, PD-1 expression has been detected on human NK cells in several cancer indications (40-43). Though NK cells exhibit cytotoxicity against many tumors, they fail to eliminate many tumors in vivo, and are frequently found in tumor beds in an inactive state. Based

363 on the collective data, we believe that PD-1 engagement is at least partially responsible for the
364 impact of PD-L1 expression by tumor cells on NK-dependent tumor rejection. However, PD-1
365 expressed by cells other than NK cells and CD8 T cells may also play a role, depending on the
366 tumor type and the nature of the immune response. The same reasoning likely applies to other
367 checkpoint receptors, including LAG-3, TIM-3 and TIGIT, that probably play a wider role in the
368 tumor microenvironment than inhibiting T cells.

369 Functional and phenotypic tests showed that the PD-1^{+} NK cells had the highest functional
370 activity when stimulated ex vivo and were largely included in the subsets of NK cells that
371 expressed activation markers (CD69 and Sca-1). These data suggest that PD-1+ NK cells are not
372 necessarily anergic in PD-L1+ tumors but may instead be inhibited in killing tumor cells. Studies
373 suggest that anergy and PD-1 expression are independent processes in T cells as well (67) and it
374 was recently reported that activation, rather than exhaustion, drives expression of PD-1 and other
375 checkpoint receptors on human T cells (68). PD-1-negative NK cells may fail to kill tumor cells
376 because they failed to become activated or have been rendered anergic. Whatever the
377 explanation, the finding that PD-1+ NK cells are the most active provides a plausible explanation
378 for why PD-L1 expression by tumor cells suppresses the response even though only a fraction of
379 NK cells expressed PD-1. Furthermore, it is consistent with the impact of PD-1 and PD-L1
380 blockade, because these more active NK cells would be expected to vigorously attack tumor cells
381 once the inhibitory interaction is disrupted.

382 PD-1 expression by CD8 T cells is also correlated with activation (68). Unexpectedly, PD-1
383 expression by NK cells occurred even within tumors that are poor targets for NK cells in vitro, such
384 as from the RMA tumor line. PD-1 expression trended higher, but not appreciably so, within tumors
385 formed from RMA transfectants that expressed NK activating ligands. The data suggest that PD-1
386 expression is induced by other activating signals or a combination of them, supplied within tumors.
387 Cytokine cocktails we have tested were not sufficient to induce PD-1 on NK cells (data not shown).

It will be important in future studies to identify the mechanisms that lead to PD-1 expression by NK cells in tumors, and the source of variation in PD-1 expression in different tumors.

Our results, and those of others (69, 70), suggest there are opportunities for combining PD-1 or PD-L1 antibody therapy with agents that enhance the anti-tumor effects of NK cells by other means including KIR blockade (71), cytokine therapy (47), ADCC (72) and other mechanisms (73) for marshaling NK cell responses against cancer. Finally, given reports that NK cells express other checkpoint receptors, such as CTLA-4, LAG-3, CD96 and TIGIT (74-76), therapies targeting those molecules may also mobilize NK responses and will be subject of future studies.

Materials and Methods:

Mice and in vivo procedures

Mice were maintained at the University of California, Berkeley or at the University of Ottawa, ON. C57BL/6J, BALB/cJ, and *Rag1*$^{-/-}$*Il2rg*$^{-/-}$ were bred from mice purchased from The Jackson Laboratory and B6-*Klrk1*$^{-/-}$ mice were described (77). *p53*$^{fl/fl}$ mice and *Kras*$^{+/LSL\text{-}G12D}$ mice, both purchased from Jackson Laboratory, were bred to generate KP (*Kras*$^{+/LSL\text{-}G12D}$*p53*$^{fl/fl}$) mice (78). Ncr1$^{+/gfp}$ mice were a gift of Dr. Mandelboim (Hebrew University, Jerusalem, Israel). For all experiments, sex- (both males and females) and age- (six- to twelve-week old) matched mice were employed.

For s.c. and orthotopic injections, tumor cells resuspended in 100 µl of RPMI without FCS were injected in the left flank or in the mammary fat pad. Tumor growth was monitored by caliper measurements. For the experimental metastasis model, tumor cells resuspended in 200 µl of RPMI without FCS were injected intra-venously in the tail vein. KP sarcomas were induced by intramuscular hind leg injection of 25,000 PFU of a lentivirus expressing Cre recombinase in a volume of 50 µl. Cre-expressing lentivirus was produced in 293T cells by simultaneous transfection

412 of a transfer vector encoding Cre (a gift from Tyler Jacks, MIT, Boston, MA) along with the
413 plasmids psPAX2 and pCMV-VSV-G. Cell culture supernatant containing Lenti-Cre was passed
414 through a 0.45 uM filter, centrifuged at 20,000 RPM, and resuspended in a 1:1 mixture of HBSS
415 and OptiMem. Viral preparations were titered using the GreenGO reporter cell line (Tyler Jacks,
416 MIT, Boston, MA).

417 To deplete CD8 T cells, mice were injected i.p. with 250 μg of monoclonal antibodies H35-
418 17.2 (specific for CD8β) or 2.43 (specific for CD8α) on day -2 and -1 relative to tumor injection.
419 CD4 T cells were depleted by i.p. injection of 500 μg of GK1.5 monoclonal antibodies (specific for
420 CD4) on days -3 and -1. To deplete NK cells in C57BL/6 mice, 250 μg of PK136 (specific for NKR-
421 P1C) were injected i.p. on day -1 and -2. In BALB/cJ mice, 10 μl of anti-asialoGM1 were injected
422 i.p. on days -2 and -1. Cell depletion was confirmed by staining peripheral blood cells with
423 antibodies different than the ones used for in vivo depletion. Specifically, NK-depletion was
424 confirmed by the absence of $CD3^{-}NKp46^{+}$ cells, CD8 T cell depletion was confirmed by the
425 absence of $CD3^{+}CD4^{-}$ cells and CD4 T cell depletion was confirmed by the absence of $CD3^{+}CD8^{-}$
426 cells.

427 For experiments using RMA-S or RMA-S-*Pdl1* cells, checkpoint blockade was performed
428 by injecting 250 μg of PD-1 (RMP1-14) or PD-L1 (10F.9G2) antibodies, or control IgG, i.p. In one
429 protocol, the antibody was delivered two days after tumor cell injection. In a second protocol, the
430 antibody was injected when the tumor volume reached 25 mm^3, and repeated two days after. In a
431 third protocol, tumor cells were injected s.c. after resuspending the cells in 100 μl of Growth Factor
432 Reduced MATRIGEL (BD) mixed with 20 μg of control or PD-1 or PD-L1 antibodies.

433 For experiments using CT26-*Pdl1-/-* cells transduced with empty vector or *Pdl1* expression
434 vector, checkpoint blockade was performed by injecting 250 μg of PD-L1 (10F.9G2) antibodies, or
435 control IgG i.p., daily from day 1 to day 10 after injecting tumor cells. In these mice, immune

depletion was performed at day -2, -1, 7 and 14. In a second protocol, PD-L1 antibody was injected at day 3, 4, 5, 7 and 10. In these animals, NK depletion was performed at day 2, 9 and 16.

Cell lines and cell culture

All cell lines were cultured at 37°C in humidified atmosphere containing 5% CO_2 with media containing 100 U/mL penicillin, 100 μg/mL streptomycin, 0.2 mg/mL glutamine, 10 μg/mL gentamycin sulfate, 20 mM Hepes and 5% FCS (10% FCS in the case of CT26 cells). RMA, RMA-*Pdl1*, RMA-S, RMA-S-*Pdl1*, RMA-*m157*, RMA-RAE-1ε, C1498, CT26, CT26-*Pdl1*$^{-/-}$, K562, K562-*Pdl1*, A20, YAC-1, YAC-1-*Pdl1*, 4T1 and 4T1-*Pdl1*$^{-/-}$ were cultured in RPMI whereas B16, B16-*Pdl1* and TRAMP-C2 were cultured in DMEM. NK92 and NK92-*Pdcd1* were cultured in MEM-α with 10% FCS, 10% Horse Serum, 100 U/ml recombinant human IL-2, 100 U/mL penicillin, 100 μg/mL streptomycin, 0.2 mg/mL glutamine, 10 μg/mL gentamycin sulfate, and 20 mM Hepes. Cell line identify was confirmed by flow cytometry or PCR and tested negative for mycoplasma.

Flow cytometry

In mice injected with tumor cells s.c., or in the sarcoma model, draining lymph nodes (inguinal), non-draining lymph nodes (brachial LN) and spleens were gently dissociated through a 40 μm filter and the resulting single cell suspensions were employed for experiments. The tumors were excised after separating the skin, cut in pieces and dissociated using a gentleMACS Dissociator (Miltenyi). In mice injected with tumor cells i.v., lungs were perfused and then dissociated using a gentleMACS Dissociator. Cell preparations from tumors and lungs were loaded on a mouse-lympholyte gradient (Cedarlane) and then stained. TRAMP and Eu-Myc derived tumors were dissociated with collagenase and cells were stored frozen at -80° C. Before staining, cells were thawed and loaded on a mouse-lympholyte gradient.

Dead cells were excluded by staining with Live-Dead fixable stain kit (Molecular Probes) for 30 min. Cells were then incubated for 20 min with 2.4G2 hybridoma supernatant to block FcγRII/III receptors and for a further 20 min primary specific antibodies, before washing. When necessary, an additional incubation with fluorochrome-conjugated streptavidin (Biolegend) was performed and the samples were subjected to flow cytometric analysis. For intracellular staining of IFN-γ and granzyme B, we used the Cytofix/Cytoperm kit (BD), following the manufacturer's instructions.

Multicolor flow cytometry was performed with an LSRFortessa (BD) or with an X20-Fortessa (BD), and data were analyzed with the FlowJo software (Tree Star Inc.).

Antibodies

For flow cytometry we used the following antibodies (clone names are in parentheses). From Biolegend: anti-CD3**ε** (145-2C11), anti-CD4 (GK1.5), anti-CD11b (M1/70), CD11c (N418), anti-CD19 (6D5), anti-CD69 (H1.2F3), anti-CD137 (4-1BB, clone 17B5), anti-DNAM (10E5), anti-F4/80 (BM8), anti-Ly6C (HK1.4), anti-Ly6G (1A8), anti-Ly49A (YE1/48.10.6), anti-NKp46 (29A1.4), anti-NKR-P1C (PK136), anti-PD-1 (29F.1A12), anti-PD-L1 (10F.9G2), anti-PVR (TX56), anti-Sca-1 (D7), anti-Ter119 (TER-119), rat-IgG2a isotype control. From eBioscience: anti-CD25 (PC61.5), anti-CD27 (37.51), anti-CD45.1 (A20), anti-CD45.2 (104), anti-Ki67 (SolA15), anti-mouse CD107a (eBio1D4B), anti-human CD107a (eBioH4A3), anti-KLRG1 (2F1), anti-Ly49G2 (LGL-1), anti-MHC class I H-2D^{b} (28.14.8), anti-MHC class I H-2K^{d} (SF1-1.1.1), anti-NKG2A/C/E (20d5), anti-NKG2D (MI-6). From BD Pharmingen: anti-CD25 (PC61), anti-Ly49I (YLI-90) and anti-granzyme B (GB11). From R&D Systems: anti-H60 (205326), anti-MULT1 (237104), anti-Nectin2 (829038) anti-pan-RAE-1 (186107). Anti-Ly49C (4LO3311) was a gift from S. Lemieux, l'Institut national de la recherche scientifique–Institut Armand-Frappier (Laval, QC). Anti-m157 (6H121) was a gift from W. Yokoyama, Washington University School of Medicine (St. Louis, MO).

Antibodies for in vivo depletions or in vivo treatments were obtained from Leinco (St. Louis, MO) except for anti-asialoGM-1 obtained from Biolegend.

Viral Transduction

A cDNA clone encoding wild type mouse *Pdl1* (gene ID 60533) was subcloned into the pQCXIN (provided by L. Coscoy, University of California, Berkeley) or MSCV-IRES-Thy1.1-DEST (Addgene 17442) retroviral expression vectors. A cDNA clone encoding wild type mouse *Pdcd1* (gene ID 18566) was subcloned into the 236pHAGE.EF1A expression vector, provided by R. Tjian at the University of California, Berkeley, CA. Cells expressing the vector were selected based on mCherry expression. *m157*-encoding plasmid was a gift of J. Sun, Memorial Sloan Kettering Cancer Center (New York, NY). Expression plasmids were amplified in DH5α bacterial cells and purified by midi-prep (Quiagen).

Retro- and lenti-viral expression vectors were generated by transfecting 293T cells with 2 μg of vector with 2 μg of packaging+polymerase-encoding plasmids using Lipofectamine 2000. Virus-containing supernatants were used to transduce target cells by spin-infection (800xg for 2 hours at 37°C) with 8 μg/ml of Polybrene. Transduced cells were sorted using an Influx cell sorter or selected by culturing them in medium containing 1 mg/ml of G418 for 48 hours, as indicated.

Generation of PD-L1-deficient mutants of the CT26 and 4T1 cell lines.

Single guide (sg) RNA targeting the third exon of the *Pdl1* gene (sequence: GTATGGCAGCAACGTCACGA) was cloned into the LentiCRISPR lentiviral backbone vector, also containing the *Cas9* gene. CT26 or 4T1 cells were transfected with 2 μg of plasmid and after 2 days were treated with 20 ng/ml of recombinant mouse IFN-γ (Peprotech). After 48 hrs, cells that failed to upregulate PD-L1 were sorted. IFN-γ treatment and cell sorting were repeated for three

cycles, after growing the cells for 5 days after each treatment. Cells were cultured extensively in the absence of IFN-γ before use.

Flow cytometry based killing assay

15,000 CFSE-labeled target cells were incubated for 5 hours with effector cells at different E:T ratios in 96 well U bottom plates in technical triplicates. Cells were then stained with the Live/Dead Fixable viability dye (Molecular probes) and resuspended in 150 μl of flow buffer. 8,000 APC-labelled microbeads (Bangs Laboratories) resuspended in 50 μl were added to each well. 180 μl of cells+beads were acquired at the flow cytometer using the HTS plate reader. The ratio among viable target cells (defined as $CFSE^{+}$viability dye^{-} cells) and fluorescent microbeads (defined as APC^{+} events) was calculated in each well (T/B). %Specific lysis was calculated for each well as:

$$\%\text{Specific lysis} = (T/B^{\text{experimental condition}} - T/B^{\text{target alone}})/(T/B^{\text{target+bleach}} - T/B^{\text{target alone}})\text{x}100$$

Degranulation assay

Splenocytes from resting *Ncr1*$^{+/gfp}$ mice (all NK cells express GFP) were spin infected twice (at day 0 and day 1) with *Pdcd1*-encoding lentivirus in the presence of 1000 U/ml of recombinant human IL-2. On day 2, activated splenocytes were harvested, stained with cell trace violet (Biolegend) and used as effectors in a degranulation assay. 30,000 effector cells were cultured with RMA-S or RMA-S-*Pdl1* cells at different T:E ratios for 5 hrs with 1 μg of Golgi Plug (BD), 1 μg of Golgi Stop (BD), and anti-CD107a. PD-1 staining was performed after the stimulation. NK cells were gated as viable-cell trace $violet^{+}GFP^{+}$.

NK92-*Pdcd1* and NK92 cells transduced with empty vector were CFSE-labeled and used as effectors in a degranulation assay. 20,000 effectors cells were stimulated with K562 or K562/*Pdl1* cells at different T:E ratios for 5 hrs with 1 μg of Golgi Stop and anti-CD107a.

In other experiments, wells of flat-bottomed high-protein-binding plates were coated with 0.5 μg of control isotype or NKp46 antibody or 5 μg of NKR-P1C antibody. ~10^6 tumor-infiltrating cells were stimulated in the presence of 100 U of recombinant human IL-2, anti-CD107a, 1 μg of Golgi Plug and 1 μg of Golgi Stop. After 5 hours, cells were harvested, stained with anti-PD-1, and degranulation and IFN-γ accumulation on PD-1+ vs PD-1- NK cells was assessed by flow cytometry.

RNA isolation, reverse transcription, and quantitative PCR

Lungs from control or from mice injected with B16 tumor variants were dissociated using a gentleMACS Dissociator and RNA was extracted using the RNeasy Mini Kit (Qiagen). RNA preparations were treated with DNase I (DNA-free Kit, Invitrogen) for 25 minutes at 37°C before retro-transcribing 1 μg of RNA using the iScript reverse transcriptase system (Bio-Rad). Quantitative real-time PCR was performed on a CFX96 thermocycler (Bio-Rad) using SSO-Fast EvaGreen Supermix (Bio-Rad). *B-actin* mRNA and *Rlt19* rRNA were used as references.

Primers sequences:

Gp100:

FW: AGCACCTGGAACCACATCTA

RV: CCAGAGGGCGTTTGTGTAGT

B-actin:

FW: AGAGGGAAATCGTGCGTGAC

RV: CAATAGTGACCTGGCCGT

*Rtl*19:

FW: GGCAGTACCCTTCCTCTTCC

RV: AGCCTGTGACTGTCCATTCC

Statistics

Statistical analysis was performed with the two-tailed unpaired (or paired when indicated) Student's *t*-tests or Mann-Whitney tests or with one- or two-way ANOVA. Survival experiments were analyzed with log-rank test. Values <0.05 were considered statistically significant. Different experimental groups were equally allocated among the same cage (5-6 mice/small cage, up to 12 mice in large cage). No experimental blinding was necessary. In all experiments, when statistical analyses were performed, the compared groups had similar variance.

Study approval:

All the experiments were reviewed and approved by the Animal Care and Use Committee at the University of California, Berkeley, (Berkeley, CA) in accordance with the guidelines of the National Institutes of Health and by the Animal Care Veterinary Services at the University of Ottawa, (Ottawa, ON) in accordance with the guidelines of the Canadian Institutes of Health Research.

Author Contributions:

MA, JH, JJH, MM, MCBD and CJN performed and analyzed the experiments. TNT, CSA, AKS, HER, TWT, LZ, AI, KEJ, NM, GAK, MWM and JCB assisted with the experiments. MA and DHR conceived of the study, designed and interpreted the experiments and prepared the manuscript. All authors critically read the manuscript.

Acknowledgements

We thank Hector Nolla, Alma Valeros and Vera Tang for help with cell sorting, Francesco Spallotta and Dr. Cencioni for help with q-PCR analyses and members of the Raulet Lab and Ardolino Lab for discussions. Dr. Giuseppe Sciumè critically read the manuscript. MA was supported by an Istituto Pasteur-Fondazione Cenci Bolognetti post-doctoral fellowship, and by a CRI Irvington Fellowship. JH and CSA were supported by summer undergraduate research fellowships from Rose Hill. TWT was supported by a Student Training in Tumor Immunology Fellowship from the Cancer Research Institute. This work was supported by NIH grants R01-CA093678 and R01-AI113041 to DHR and by a Telus Ride for Dad grant from the Prostate Cancer Fight Foundation and a CIHR project grant to MA.

References:

1. Topalian SL, Hodi FS, Brahmer JR, Gettinger SN, Smith DC, McDermott DF, et al. Safety, activity, and immune correlates of anti-PD-1 antibody in cancer. *N Engl J Med.* 2012;366(26):2443-54.
2. Brahmer JR, Tykodi SS, Chow LQ, Hwu WJ, Topalian SL, Hwu P, et al. Safety and activity of anti-PD-L1 antibody in patients with advanced cancer. *N Engl J Med.* 2012;366(26):2455-65.
3. Hamid O, Robert C, Daud A, Hodi FS, Hwu WJ, Kefford R, et al. Safety and tumor responses with lambrolizumab (anti-PD-1) in melanoma. *N Engl J Med.* 2013;369(2):134-44.
4. Callahan MK, Postow MA, and Wolchok JD. CTLA-4 and PD-1 Pathway Blockade: Combinations in the Clinic. *Frontiers in oncology.* 2014;4:385.
5. Robert C, Ribas A, Wolchok JD, Hodi FS, Hamid O, Kefford R, et al. Anti-programmed-death-receptor-1 treatment with pembrolizumab in ipilimumab-refractory advanced melanoma: a randomised dose-comparison cohort of a phase 1 trial. *Lancet.* 2014;384(9948):1109-17.
6. Tumeh PC, Harview CL, Yearley JH, Shintaku IP, Taylor EJ, Robert L, et al. PD-1 blockade induces responses by inhibiting adaptive immune resistance. *Nature.* 2014;515(7528):568-71.
7. Herbst RS, Soria JC, Kowanetz M, Fine GD, Hamid O, Gordon MS, et al. Predictive correlates of response to the anti-PD-L1 antibody MPDL3280A in cancer patients. *Nature.* 2014;515(7528):563-7.
8. Powles T, Eder JP, Fine GD, Braiteh FS, Loriot Y, Cruz C, et al. MPDL3280A (anti-PD-L1) treatment leads to clinical activity in metastatic bladder cancer. *Nature.* 2014;515(7528):558-62.

9. Robert C, Long GV, Brady B, Dutriaux C, Maio M, Mortier L, et al. Nivolumab in previously untreated melanoma without BRAF mutation. *N Engl J Med.* 2015;372(4):320-30.
10. Garrido F, and Algarra I. MHC antigens and tumor escape from immune surveillance. *Adv Cancer Res.* 2001;83:117-58.
11. Aptsiauri N, Cabrera T, Garcia-Lora A, Lopez-Nevot MA, Ruiz-Cabello F, and Garrido F. MHC class I antigens and immune surveillance in transformed cells. *Int Rev Cytol.* 2007;256:139-89.
12. Ansell SM, Lesokhin AM, Borrello I, Halwani A, Scott EC, Gutierrez M, et al. PD-1 blockade with nivolumab in relapsed or refractory Hodgkin's lymphoma. *N Engl J Med.* 2015;372(4):311-9.
13. Ansell SM. Hodgkin lymphoma: MOPP chemotherapy to PD-1 blockade and beyond. *Am J Hematol.* 2016;91(1):109-12.
14. Zaretsky JM, Garcia-Diaz A, Shin DS, Escuin-Ordinas H, Hugo W, Hu-Lieskovan S, et al. Mutations Associated with Acquired Resistance to PD-1 Blockade in Melanoma. *N Engl J Med.* 2016;375(9):819-29.
15. Smahel M. PD-1/PD-L1 Blockade Therapy for Tumors with Downregulated MHC Class I Expression. *Int J Mol Sci.* 2017;18(6).
16. Aust S, Felix S, Auer K, Bachmayr-Heyda A, Kenner L, Dekan S, et al. Absence of PD-L1 on tumor cells is associated with reduced MHC I expression and PD-L1 expression increases in recurrent serous ovarian cancer. *Sci Rep.* 2017;7:42929.
17. McGranahan N, Rosenthal R, Hiley CT, Rowan AJ, Watkins TBK, Wilson GA, et al. Allele-Specific HLA Loss and Immune Escape in Lung Cancer Evolution. *Cell.* 2017;171(6):1259-71 e11.
18. Marty R, Kaabinejadian S, Rossell D, Slifker MJ, van de Haar J, Engin HB, et al. MHC-I Genotype Restricts the Oncogenic Mutational Landscape. *Cell.* 2017;171(6):1272-83 e15.
19. Roemer MG, Advani RH, Redd RA, Pinkus GS, Natkunam Y, Ligon AH, et al. Classical Hodgkin Lymphoma with Reduced beta2M/MHC Class I Expression Is Associated with Inferior Outcome Independent of 9p24.1 Status. *Cancer Immunol Res.* 2016;4(11):910-6.
20. Vivier E, Raulet DH, Moretta A, Caligiuri MA, Zitvogel L, Lanier LL, et al. Innate or adaptive immunity? The example of natural killer cells. *Science.* 2011;331(6013):44-9.
21. Marcus A, Gowen BG, Thompson TW, Iannello A, Ardolino M, Deng W, et al. Recognition of tumors by the innate immune system and natural killer cells. *Adv Immunol.* 2014;122:91-128.
22. Ruggeri L, Capanni M, Casucci M, Volpi I, Tosti A, Perruccio K, et al. Role of natural killer cell alloreactivity in HLA-mismatched hematopoietic stem cell transplantation. *Blood.* 1999;94(1):333-9.
23. Giebel S, Locatelli F, Lamparelli T, Velardi A, Davies S, Frumento G, et al. Survival advantage with KIR ligand incompatibility in hematopoietic stem cell transplantation from unrelated donors. *Blood.* 2003;102(3):814-9.
24. Beelen DW, Ottinger HD, Ferencik S, Elmaagacli AH, Peceny R, Trenschel R, et al. Genotypic inhibitory killer immunoglobulin-like receptor ligand incompatibility enhances the long-term antileukemic effect of unmodified allogeneic hematopoietic stem cell transplantation in patients with myeloid leukemias. *Blood.* 2005;105(6):2594-600.

25. Verheyden S, Schots R, Duquet W, and Demanet C. A defined donor activating natural killer cell receptor genotype protects against leukemic relapse after related HLA-identical hematopoietic stem cell transplantation. *Leukemia.* 2005;19(8):1446-51.
26. Miller JS, Cooley S, Parham P, Farag SS, Verneris MR, McQueen KL, et al. Missing KIR ligands are associated with less relapse and increased graft-versus-host disease (GVHD) following unrelated donor allogeneic HCT. *Blood.* 2007;109(11):5058-61.
27. Kim HJ, Choi Y, Min WS, Kim TG, Cho BS, Kim SY, et al. The activating killer cell immunoglobulin-like receptors as important determinants of acute graft-versus host disease in hematopoietic stem cell transplantation for acute myelogenous leukemia. *Transplantation.* 2007;84(9):1082-91.
28. Willemze R, Rodrigues CA, Labopin M, Sanz G, Michel G, Socie G, et al. KIR-ligand incompatibility in the graft-versus-host direction improves outcomes after umbilical cord blood transplantation for acute leukemia. *Leukemia.* 2009;23(3):492-500.
29. Giebel S, Nowak I, Dziaczkowska J, Czerw T, Wojnar J, Krawczyk-Kulis M, et al. Activating killer immunoglobulin-like receptor incompatibilities enhance graft-versus-host disease and affect survival after allogeneic hematopoietic stem cell transplantation. *Eur J Haematol.* 2009;83(4):343-56.
30. Cooley S, Weisdorf DJ, Guethlein LA, Klein JP, Wang T, Le CT, et al. Donor selection for natural killer cell receptor genes leads to superior survival after unrelated transplantation for acute myelogenous leukemia. *Blood.* 2010;116(14):2411-9.
31. Malmberg KJ, Carlsten M, Bjorklund A, Sohlberg E, Bryceson YT, and Ljunggren HG. Natural killer cell-mediated immunosurveillance of human cancer. *Semin Immunol.* 2017.
32. Coca S, Perez-Piqueras J, Martinez D, Colmenarejo A, Saez MA, Vallejo C, et al. The prognostic significance of intratumoral natural killer cells in patients with colorectal carcinoma. *Cancer.* 1997;79(12):2320-8.
33. Ishigami S, Natsugoe S, Tokuda K, Nakajo A, Che X, Iwashige H, et al. Prognostic value of intratumoral natural killer cells in gastric carcinoma. *Cancer.* 2000;88(3):577-83.
34. Villegas FR, Coca S, Villarrubia VG, Jimenez R, Chillon MJ, Jareno J, et al. Prognostic significance of tumor infiltrating natural killer cells subset CD57 in patients with squamous cell lung cancer. *Lung cancer.* 2002;35(1):23-8.
35. Schleypen JS, Baur N, Kammerer R, Nelson PJ, Rohrmann K, Grone EF, et al. Cytotoxic markers and frequency predict functional capacity of natural killer cells infiltrating renal cell carcinoma. *Clinical cancer research : an official journal of the American Association for Cancer Research.* 2006;12(3 Pt 1):718-25.
36. McKay K, Moore PC, Smoller BR, and Hiatt KM. Association between natural killer cells and regression in melanocytic lesions. *Hum Pathol.* 2011;42(12):1960-4.
37. Pasero C, Gravis G, Granjeaud S, Guerin M, Thomassin-Piana J, Rocchi P, et al. Highly effective NK cells are associated with good prognosis in patients with metastatic prostate cancer. *Oncotarget.* 2015;6(16):14360-73.
38. Shifrin N, Raulet DH, and Ardolino M. NK cell self tolerance, responsiveness and missing self recognition. *Semin Immunol.* 2014;26(2):138-44.
39. Iannello A, Thompson TW, Ardolino M, Marcus A, and Raulet DH. Immunosurveillance and immunotherapy of tumors by innate immune cells. *Current opinion in immunology.* 2015;38:52-8.
40. Benson DM, Jr., Bakan CE, Mishra A, Hofmeister CC, Efebera Y, Becknell B, et al. The PD-1/PD-L1 axis modulates the natural killer cell versus multiple myeloma effect: a

therapeutic target for CT-011, a novel monoclonal anti-PD-1 antibody. *Blood.* 2010;116(13):2286-94.
41. Beldi-Ferchiou A, Lambert M, Dogniaux S, Vely F, Vivier E, Olive D, et al. PD-1 mediates functional exhaustion of activated NK cells in patients with Kaposi sarcoma. *Oncotarget.* 2016.
42. Pesce S, Greppi M, Tabellini G, Rampinelli F, Parolini S, Olive D, et al. Identification of a subset of human natural killer cells expressing high levels of programmed death 1: A phenotypic and functional characterization. *J Allergy Clin Immunol.* 2017;139(1):335-46 e3.
43. Liu Y, Cheng Y, Xu Y, Wang Z, Du X, Li C, et al. Increased expression of programmed cell death protein 1 on NK cells inhibits NK-cell-mediated anti-tumor function and indicates poor prognosis in digestive cancers. *Oncogene.* 2017.
44. Vari F, Arpon D, Keane C, Hertzberg MS, Talaulikar D, Jain S, et al. Immune evasion via PD-1/PD-L1 on NK cells and monocyte/macrophages is more prominent in Hodgkin lymphoma than DLBCL. *Blood.* 2018;131(16):1809-19.
45. Karre K, Ljunggren HG, Piontek G, and Kiessling R. Selective rejection of H-2-deficient lymphoma variants suggests alternative immune defense strategy. *Nature.* 1986;319:675-8.
46. Matsumoto K, Morisaki T, Kuroki H, Kubo M, Onishi H, Nakamura K, et al. Exosomes secreted from monocyte-derived dendritic cells support in vitro naive CD4+ T cell survival through NF-(kappa)B activation. *Cellular immunology.* 2004;231(1-2):20-9.
47. Ardolino M, Azimi CS, Iannello A, Trevino TN, Horan L, Zhang L, et al. Cytokine therapy reverses NK cell anergy in MHC-deficient tumors. *J Clin Invest.* 2014;124(11):4781-94.
48. Seaman WE, Sleisenger M, Eriksson E, and Koo GC. Depletion of natural killer cells in mice by monoclonal antibody to NK-1.1. Reduction in host defense against malignancy without loss of cellular or humoral immunity. *J Immunol.* 1987;138(12):4539-44.
49. Sorensen MR, Pedersen SR, Lindkvist A, Christensen JP, and Thomsen AR. Quantification of B16 melanoma cells in lungs using triplex Q-PCR--a new approach to evaluate melanoma cell metastasis and tumor control. *PLoS One.* 2014;9(1):e87831.
50. Castle JC, Loewer M, Boegel S, de Graaf J, Bender C, Tadmor AD, et al. Immunomic, genomic and transcriptomic characterization of CT26 colorectal carcinoma. *BMC Genomics.* 2014;15:190.
51. Chiossone L, Chaix J, Fuseri N, Roth C, Vivier E, and Walzer T. Maturation of mouse NK cells is a 4-stage developmental program. *Blood.* 2009;113(22):5488-96.
52. Joncker NT, Fernandez NC, Treiner E, Vivier E, and Raulet DH. NK cell responsiveness is tuned commensurate with the number of inhibitory receptors for self-MHC class I: the rheostat model. *J Immunol.* 2009;182(8):4572-80.
53. Joncker NT, Shifrin N, Delebecque F, and Raulet DH. Mature natural killer cells reset their responsiveness when exposed to an altered MHC environment. *J Exp Med.* 2010;207(10):2065-72.
54. Elliott JM, Wahle JA, and Yokoyama WM. MHC class I-deficient natural killer cells acquire a licensed phenotype after transfer into an MHC class I-sufficient environment. *J Exp Med.* 2010;207(10):2073-9.
55. Huang AC, Postow MA, Orlowski RJ, Mick R, Bengsch B, Manne S, et al. T-cell invigoration to tumour burden ratio associated with anti-PD-1 response. *Nature.* 2017;545(7652):60-5.
56. Martincorena I, and Campbell PJ. Somatic mutation in cancer and normal cells. *Science.* 2015;349(6255):1483-9.

57. Van Allen EM, Miao D, Schilling B, Shukla SA, Blank C, Zimmer L, et al. Genomic correlates of response to CTLA-4 blockade in metastatic melanoma. *Science.* 2015;350(6257):207-11.
58. Diaz LA, Jr., and Le DT. PD-1 Blockade in Tumors with Mismatch-Repair Deficiency. *N Engl J Med.* 2015;373(20):1979.
59. McGranahan N, Furness AJ, Rosenthal R, Ramskov S, Lyngaa R, Saini SK, et al. Clonal neoantigens elicit T cell immunoreactivity and sensitivity to immune checkpoint blockade. *Science.* 2016;351(6280):1463-9.
60. Garrido F, Cabrera T, Lopez-Nevot MA, and Ruiz-Cabello F. HLA class I antigens in human tumors. *Adv Cancer Res.* 1995;67:155-95.
61. Raulet DH, and Guerra N. Oncogenic stress sensed by the immune system: role of natural killer cell receptors. *Nat Rev Immunol.* 2009;9(8):568-80.
62. Paschen A, Baingo J, and Schadendorf D. Expression of stress ligands of the immunoreceptor NKG2D in melanoma: regulation and clinical significance. *Eur J Cell Biol.* 2014;93(1-2):49-54.
63. Zhang J, Basher F, and Wu JD. NKG2D Ligands in Tumor Immunity: Two Sides of a Coin. *Front Immunol.* 2015;6:97.
64. Fionda C, Soriani A, Zingoni A, Santoni A, and Cippitelli M. NKG2D and DNAM-1 Ligands: Molecular Targets for NK Cell-Mediated Immunotherapeutic Intervention in Multiple Myeloma. *Biomed Res Int.* 2015;2015:178698.
65. Zingoni A, Fionda C, Borrelli C, Cippitelli M, Santoni A, and Soriani A. Natural Killer Cell Response to Chemotherapy-Stressed Cancer Cells: Role in Tumor Immunosurveillance. *Front Immunol.* 2017;8:1194.
66. Gordon SR, Maute RL, Dulken BW, Hutter G, George BM, McCracken MN, et al. PD-1 expression by tumour-associated macrophages inhibits phagocytosis and tumour immunity. *Nature.* 2017;545(7655):495-9.
67. Schietinger A, Philip M, Krisnawan VE, Chiu EY, Delrow JJ, Basom RS, et al. Tumor-Specific T Cell Dysfunction Is a Dynamic Antigen-Driven Differentiation Program Initiated Early during Tumorigenesis. *Immunity.* 2016;45(2):389-401.
68. Legat A, Speiser DE, Pircher H, Zehn D, and Fuertes Marraco SA. Inhibitory Receptor Expression Depends More Dominantly on Differentiation and Activation than "Exhaustion" of Human CD8 T Cells. *Front Immunol.* 2013;4:455.
69. Terme M, Ullrich E, Aymeric L, Meinhardt K, Desbois M, Delahaye N, et al. IL-18 induces PD-1-dependent immunosuppression in cancer. *Cancer Res.* 2011;71(16):5393-9.
70. Mittal D, Young A, Stannard K, Yong M, Teng MW, Allard B, et al. Antimetastatic effects of blocking PD-1 and the adenosine A2A receptor. *Cancer Res.* 2014;74(14):3652-8.
71. Romagne F, Andre P, Spee P, Zahn S, Anfossi N, Gauthier L, et al. Preclinical characterization of 1-7F9, a novel human anti-KIR receptor therapeutic antibody that augments natural killer-mediated killing of tumor cells. *Blood.* 2009;114(13):2667-77.
72. Kohrt HE, Houot R, Weiskopf K, Goldstein MJ, Scheeren F, Czerwinski D, et al. Stimulation of natural killer cells with a CD137-specific antibody enhances trastuzumab efficacy in xenotransplant models of breast cancer. *J Clin Invest.* 2012;122(3):1066-75.
73. Deng W, Gowen BG, Zhang L, Wang L, Lau S, Iannello A, et al. Antitumor immunity. A shed NKG2D ligand that promotes natural killer cell activation and tumor rejection. *Science.* 2015;348(6230):136-9.

74. Triebel F, Jitsukawa S, Baixeras E, Roman-Roman S, Genevee C, Viegas-Pequignot E, et al. LAG-3, a novel lymphocyte activation gene closely related to CD4. *Journal of Experimental Medicine.* 1990;171(5):1393-405.
75. Stojanovic A, Fiegler N, Brunner-Weinzierl M, and Cerwenka A. CTLA-4 is expressed by activated mouse NK cells and inhibits NK Cell IFN-gamma production in response to mature dendritic cells. *J Immunol.* 2014;192(9):4184-91.
76. Chan CJ, Martinet L, Gilfillan S, Souza-Fonseca-Guimaraes F, Chow MT, Town L, et al. The receptors CD96 and CD226 oppose each other in the regulation of natural killer cell functions. *Nat Immunol.* 2014;15(5):431-8.
77. Guerra N, Tan YX, Joncker NT, Choy A, Gallardo F, Xiong N, et al. NKG2D-deficient mice are defective in tumor surveillance in models of spontaneous malignancy. *Immunity.* 2008;28(4):571-80.
78. Kirsch DG, Dinulescu DM, Miller JB, Grimm J, Santiago PM, Young NP, et al. A spatially and temporally restricted mouse model of soft tissue sarcoma. *Nat Med.* 2007;13(8):992-7.

Figure Legends:

Figure 1: Therapeutic anti-tumor effect of PD-1 or PD-L1 antibodies, dependent on NK cells.

(A) NK, CD4 and/or CD8 T cells were depleted before s.c. injection of 10^6 RMA-S cells. Tumor volumes (means±S.E.) are shown. The experiments depicted are representative of two performed. n=4-5/group. Statistical analyses with two-way ANOVA test.

(B) PD-L1 expression was analyzed on cells stimulated or not with 20 ng/ml of IFN-γ for 48 hours. Representative of 3 performed.

(C) 2x10^6 RMA-S or RMA-S-*Pdl1* cells (naturally expressing CD45.2) or TRAMP-C2 cells (transduced with Thy1.1) were injected s.c. into C57BL/6-CD45.1$^+$ mice, and PD-L1 expression was analyzed on splenic or intratumoral cells, gating on dendritic cells (viable-CD45.1$^+$CD3$^-$CD19$^-$ Ter119$^-$NK1.1$^-$CD11b$^+$Ly6G$^-$CD11c^{high}), monocytes (viable-CD45.1$^+$CD3$^-$CD19$^-$Ter119$^-$NK1.1$^-$ CD11b$^+$Ly6G$^-$CD11c$^-$Ly6C$^+$), and tumor cells (viable-CD45.1$^-$CD45.2$^+$ cells for RMA-S and RMA-S-*Pdl1,* or viable-CD45.2$^-$Thy1.1$^+$ for TRAMP-C2). The MFI of isotype control-stained cells was subtracted from the MFI of PD-L1-stained cells. Two experiments were pooled (n=5-7/group).

(D) 10^6 RMA-S-*Pdl1* cells were injected in mice depleted of NK, CD8 or CD4 T cells. Tumor

volumes (means±S.E.) are shown. Representative of two performed. n=4-5/group. Statistical analyses with two-way ANOVA test.

(E) 10^6 RMA-S-*Pdl1* cells were injected in C57BL/6 mice and after two days 250 µg of PD-1 or control antibody were administered. Some mice were depleted of NK cells two days before tumor cell injection. In the figure, we pooled data from 2 of the 3 experiments performed, n=6-11/group. Statistical analyses with two-way ANOVA tests. Both NK-depleted groups were significantly different than the corresponding undepleted groups.

(F) 10^6 RMA-S-*Pdl1* cells were injected and tumors were allowed to grow to an average of 25 mm^3, at which time (and two days later) the mice were treated with 250 µg of PD-1 antibody or cIg. Representative of 2 performed, n=5/group. Statistical analyses with two-way ANOVA tests.

(G-H) $0.5x10^6$ RMA-S-*Pdl1* tumor cells were mixed with Matrigel and either 20 µg of anti-PD-1 or control Ig **(E, G)** or anti-PD-L1 or control Ig **(F, H)** and injected s.c.. in C57BL/6 mice. Experiments were repeated at least two times, with n=4-5/group. Statistical analyses with two-way ANOVA tests.

Figure 2: PD-1 is expressed on tumor infiltrating NK cells and suppresses NK cell cytotoxicity in vitro.

(A-B) C57BL/6 mice were injected s.c. with $2x10^6$ RMA-S cells or PBS; BALB/cJ mice were injected with $0.5x10^6$ CT26 cells. PD-1 expression was assessed after 13 days on NK cells from spleens, axillary lymph nodes, inguinal lymph nodes and tumors. Staining for PD-1 (dark-grey filled histograms) or control IgG (light-grey filled histograms) is shown. NK cells were gated as viable-$Ter119^-CD3^-CD19^-F4/80^-NKp46^+$ cells in BALB/cJ, or $Ter119^-CD3^-CD19^-F4/80^-NKp46^+NK1.1^+$ cells in C57BL/6 mice. Representative of six experiments performed with n=3-5.

(C) Summary of PD-1 expression on intratumoral NK and CD8+ T cells in mice injected with RMA, RMA-S, B16, C1498, CT26, 4T1 or A20 cells, or on intratumoral NK cells in the prostates or thymi

852 from spontaneous cancer models (TRAMP and Eu-Myc models, respectively), or in KP sarcomas.
853 PD-1 expression on NK cells in each model was assessed in at least 3 independent experiments,
854 with at least n=3.
855 **(D-E)** IL-2-activated NK cells previously transduced with a *Pdcd1* expression vector were
856 stimulated with RMA-S or RMA-S-*Pdl1* cells at different target to effector (T:E) ratios before
857 determining degranulation **(D)** and IFN-γ production **(E)** of PD-1$^+$ NK cells. The experiments
858 depicted are representative of 3 performed. Every T:E ratio is the average$\pm$S.D. of 3 technical
859 replicates. Statistical analysis employed two-way ANOVA.
860 **(F-G)** NK92 cells transduced with *Pdcd1* (*Pdcd1* encodes PD-1) or an empty vector, were
861 stimulated with K562 or K562-*Pdl1* cells and lysis of target cells **(F)** or degranulation of effector
862 cells **(G)** was assessed by flow cytometry. F and G are representative of 4 and 2 experiments
863 performed, respectively. Every T:E ratio is the average of 3 technical replicates. Statistical analysis
864 employed two-way ANOVA with repeated measures.
865
866 **Figure 3: Expression of PD-L1 by NK cell-sensitive, T cell-resistant tumor cells promotes**
867 **more aggressive tumor growth in vivo.**
868 **(A)** RMA-S cells were transduced with a PD-L1 expression or an empty control vector. G418-
869 resistant transductants were selected. Transduced cells, as well as untransduced RMA-S cells,
870 were injected in C57BL/6 mice (10^6 cells/mouse s.c.) and tumor growth was monitored. Tumor
871 volumes (means ± S.E.) are shown for each time-point. The experiment shown is representative of
872 3 performed, n=5-6. Statistical analyses with two-way ANOVA (*: $p<0.05$).
873 Survival **(B)** and in vivo tumor growth (means±SE) **(C)** were assessed after s.c. injection of $1x10^6$
874 RMA-S or RMA-S-*Pdl1* tumor cells in C57BL/6 mice. Where indicated, NK cells were depleted by
875 injecting NK1.1 antibody. The results depicted were representative of 8 independent experiments,

two of which included NK cell-depleted mice for comparison. In the experiment shown, n=6-7 per group. Statistical analyses were performed in A with the log-rank (Mantel-Cox) test and in B with a two-way ANOVA test (**: $p<0.01$).

(D) 10^6 RMA-S or RMA-S-*Pdl1* cells were injected s.c. into *Rag1*$^{-/-}$*Il2rg*$^{-/-}$ mice, and tumor growth was assessed. Tumor volumes (means±S.E.) are shown. The experiment shown is representative of 3 independent experiments, n=4/group.

(E) 10^6 RMA or RMA-*Pdl1* tumor cells were injected s.c. into C57BL/6 mice and tumor growth was monitored. Tumor volumes (means±S.E.) are shown. The experiment shown is representative of two performed. n=5 for RMA group and 6 for RMA-*Pdl1* group.

Figure 4: PD-1 suppresses NK cell-mediated control of B16 colonization in the lungs.

(A) B16-BL6 cells were transduced with a retroviral vector encoding mouse PD-L1, and sorted for PD-L1 expression, which is depicted.

(B) C57BL/6 mice were injected i.v. with $0.25x10^6$ B16-BL6 tumor cells or saline solution. When mice were terminally ill, PD-1 expression was assessed by flow cytometry on splenic or lung NK cells. NK cells were gated as viable-CD45$^+$Ter119$^-$CD3$^-$CD19$^-$F4/80$^-$NK1.1$^+$NKp46$^+$. In E: n=3 for the control group and 11 for B16 group. Statistical analyses with a Student's t-test.

(C-F) Kaplan-Meier analyses of C57BL/6 mice injected i.v. with 5,000 (C-D) or 20,000 (E-F) B16 or B16-*Pdl1* cells. In D and F, mice were NK-depleted with NK1.1 antibody. C and D represent results pooled from 2 experiments, with n=7-15/group. E and F: results pooled from 2 experiments, with n=8-12/combined group. Statistical analyses with the log-rank (Mantel-Cox) test.

(G) C57BL/6 mice were injected i.v. with $2x10^4$ B16 or B16-*Pdl1* cells. 21 days later, the presence of tumors in the lungs was assessed by macroscopic examination. Data from the combination of two independent experiments with n=12-13/ combined group; statistical analysis with Fisher's exact test.

(H) C57BL/6 mice were injected i.v. with 20,000 B16 or B16-*Pdl1* cells. 21 days later, tumors burden in the lungs was assessed by q-RT-PCR of transcripts of the melanoma-specific gene *Gp100*. H is the combination of two independent experiments with n=9-10/group; statistical analysis with Mann-Whitney test.

Figure 5: PD-L1 expression by CT26 tumor cells prevents tumor rejection mediated by NK cells and CD8 T cells.

(A) PD-L1 expression by CT26 cell variants. Cells were untreated or treated with 20 ng/ml of IFN-γ for 48 hrs and PD-L1 expression was analyzed by flow cytometry. Top panel: Comparison of CT26 and CT26-*Pdl1-/-* cells. Lower panel: Comparison of CT26-*Pdl1-/-* cells transduced with a PD-L1 expression vector or with an empty vector. Wildtype CT26 cells transduced with empty vector served as a control.

(B, C) In vivo growth of CT26 or CT26-*Pdl1-/-* tumors was assessed after s.c. injection of $0.5x10^6$ cells in BALB/cJ mice. Some mice were depleted of NK cells (with asialoGM-1 antibody), CD8 T cells (with CD8α-specific 2.43 antibody), or both, before tumor cell injection. Tumor volumes (means±S.E.) are shown. In panel B: two-way ANOVA tests were used to compare CT26-*Pdl1*$^{-/-}$ /undepleted mice to either CT26/undepleted mice ($p<0.01$), CT26-*Pdl1*$^{-/-}$/NK-depleted mice ($p<0.0001$), or CT26-*Pdl1*$^{-/-}$/CD8-depleted mice ($p<0.01$). Two-way ANOVA tests were also used to compare CT26-*Pdl1*$^{-/-}$/NK&CD8-depleted mice to either CT26-*Pdl1*$^{-/-}$ /CD8-depleted mice ($p<0.05$) or CT26-*Pdl1*$^{-/-}$/NK-depleted mice ($p=0.0599$). In panel C, none of the differences were significant. Data from B and C are from the same experiment, which is representative of 2 performed. n=8 for the experiment shown.

(D) $0.2x10^6$ CT26-*Pdl1-/-* cells transduced with an empty vector or a PD-L1 expression vector, or CT26 wild type cells transduced with an empty vector, were injected s.c. in BALB/cJ mice and

tumor progression was assessed. The experiment depicted is representative of 3 performed, n=3-4 mice/group. Statistical analyses with two-way ANOVA tests (*: $p<0.05$ and ***: $p<0.001$).

Figure 6: NK cells are necessary to mediate full therapeutic efficacy of PD-L1 blockade in the T cell-sensitive CT26 tumor model.

(A) Mice were injected with $0.2x10^6$ CT26-*Pdl1-/-* cells transduced with an empty vector or a PD-L1 expression vector and treated with 250 μg of anti-PD-L1 or control Ig daily for 10 days by i.p. injection. Statistical analyses with two-way ANOVA tests (*:$p<0.05$ and **:$p<0.01$). n=4-5 mice/group. Representative of 3 performed.

(B) $0.2x10^6$ CT26-*Pdl1-/-* cells transduced with a PD-L1 expression vector were injected in BALB/cJ mice. Where indicated, NK or CD8 T cells were depleted by i.p. injection of anti-asialoGM1 or 2.43 antibodies two and one days before tumor injection. Mice were treated with 250 μg of anti-PD-L1 or control Ig daily for 10 days by i.p. injection. n=4-5 mice/group. Representative of 3 performed. Statistical analyses with Mann-Whitney tests comparing the anti-PD-L1 group with the other experimental groups at days 15, 17 and 19 (*:$p<0.05$ for all such comparisons).

(C) BALB/cJ mice were injected $0.25x10^6$ CT26-*Pdl1-/-* +*Pdl1* cells. PD-L1 or cIg antibodies were injected 3, 4, 5, 7 and 12 days after tumor injection. Some mice were NK-depleted 2, 9 and 16 days after tumor injection. n=6-9 mice/group. Data from the combination of two independent experiments. Statistical analysis with Two-way ANOVA with repeated measurements. **:$p<0.01$.

(D) 500,000 cells comprising a 1:1 mixture of CT26-*Pdl1-/-* +*Pdl1-IRES-Thy1.1* and CT26-*Pdl1-/-* +*empty-IRES-Thy1.1* cells were injected in BALB/cJ mice depleted or not of NK cells. Tumors were analyzed by flow cytometry as soon as they become palpable. Tumor cells were identified as CD45-Thy1.1+. Representative of 3 performed, n=3/group, statistical analysis with two tailed paired Student's t-test.

(E) 0.2x10^6 CT26 or CT26-*Pdl1-/-* cells were injected s.c. in BALB/cJ mice. Once tumors were established, mice were treated with 250 μg/day of PD-L1 or control antibody for 2 days and intracellular granzyme B expression was assessed in PD-1$^+$ or PD-1-negative tumor-infiltrating NK cells. Representative of 2 performed. n=3-5 mice/group. Statistical analysis with two-tailed unpaired Student's t-tests, *: $p<0.05$.

Figure 7: PD-1 engagement suppresses NK cell responses to 4T1 orthotopic tumors.

(A) 4T1 or 4T1-*Pdl1-/-* cells were stimulated or not with IFN-γ and PD-L1 expression was analyzed by flow cytometry.

(B-E) 100,000 tumor cells were injected in the mammary fat pad of BALB/cJ mice. Where indicated, mice were immune-depleted two and one days before tumor injection, and then 7 and 14 days after tumor injection. Results from B and C come from the same experiment. Results from D and E come from the same experiment. n=7-8 mice/group. The two experiments are representative of 3 performed. Statistical analysis with two-way ANOVA with repeated measurements comparing every group with 4T1-*Pdl1-/-* undepleted (in B and D) or with 4T1 undepleted (in C and E). *: $p<0.05$; **: $p<0.01$; ****: $p<0.00001$.

Figure 8: PD-1 is upregulated on the most activated tumor infiltrating NK cells.

(A) PD-1 expression on different NK cell maturation subsets in RMA-S tumors. R0-R3 stages as follows: R0=CD27$^-$CD11b$^-$; R1=CD27$^+$CD11b$^-$; R2=CD27$^+$CD11b$^+$; R3=CD27$^-$CD11b$^+$. 3 independent experiments were pooled (n=7-18/combined group). Statistical analysis with one-way ANOVA with repeated measures.

(B) NK cells from RMA-S tumors were stained with antibodies for Ly49I, Ly49C, and NKG2A and PD-1 expression was assessed on the three populations by flow cytometry. C$^+$I$^+$N$^+$ cells expressed

all the receptors; $C^+ \pm I^+ \pm N^+$ cells expressed at least one of the receptors; $C^-I^-N^-$ NK cells lacked expression of all three receptors. Data from 2 independent experiments are included. Statistical analysis with one-way ANOVA with repeated measures.

NK cells from RMA-S **(C)**, CT26 **(D)** or KP Sarcoma **(E)** tumors were co-stained with PD-1 antibody and antibody against Sca-1 or CD69. PD-1 expression was assessed by flow cytometry on gated NK cells that did, or did not, express such markers. Representative contour plots and summary of the data are depicted. In C and E, 3 independent experiments were pooled; in D, 2 independent experiments were pooled; n=6-15. Statistical analysis with two tailed paired Student's t-tests.

Figure 9: In RMA-S tumors PD-1$^+$ NK cells are more functionally responsive than PD-1-negative NK cells.

NK cells from RMA-S-*Pdl1* **(A)** or RMA-S **(B)** derived tumors were stimulated with plate-bound isotype control, anti-NKp46 or anti-NKR-P1C, and degranulation and IFN-γ accumulation of PD-1$^+$ vs. PD-1$^-$ NK cells was assessed. Representative of two experiments performed. n=4-5. Statistical analyses with two-tailed paired Student's t-tests.

Figure 10: In CT26 tumors PD-1$^+$ NK cells are more responsive than PD-1-negative NK cells.

NK cells from tumors deriving from CT26-Pdl1-/- cells reconstituted with PD-L1 **(A)** or an empty vector **(B)** were stimulated with plate-bound isotype control or anti-NKp46 or PMA/I. Degranulation and IFN-γ accumulation of PD-1$^+$ vs. PD-1$^-$ NK cells were assessed. Representative of two experiments performed. n=4. Statistical analyses with two-tailed paired Student's t-tests.

Supplementary Figure 1: In vivo establishment of B16 tumors is delayed by NK cells but not

CD8 T cells.

Kaplan-Meier analyses of C57BL/6 mice injected i.v. with 20,000 B16 or B16-*Pdl1* cells. Some mice were depleted of CD8 and NK cells. n=4-5/group.

Supplementary Figure 2: Expression of NK-activating ligands on tumor cell lines.

CT26, 4T1, RMA-S and B16 cells were stained with control isotypes (red histograms) or antibodies specific for H60, MULT1, pan-RAE-1, PVR or Nectin-2 (blue lines). Data are representative of two experiments performed with similar outcomes.

Supplementary Figure 3: Engagement of activating receptors by tumor cells does not induce higher PD-1 expression on tumor-infiltrating NK cells.

(A) NK cells from RMA or RMA-*m157* s.c. tumors were stained for Ly49H and PD-1, and PD-1 expression was analyzed on Ly49H^{+} NK cells. **(B)** NK cells from RMA-RAE-1 s.c. tumors in wildtype mice or *Klrk1*$^{-/-}$ mice (lacking expression of NKG2D) were stained with PD-1 antibody. A is representative of two experiments performed. In B, two experiments were combined. In A, n=5/group; in B, n=11/group. In A, statistical analyses with two-tailed unpaired Student's t-tests; in B with Mann-Whitney test.

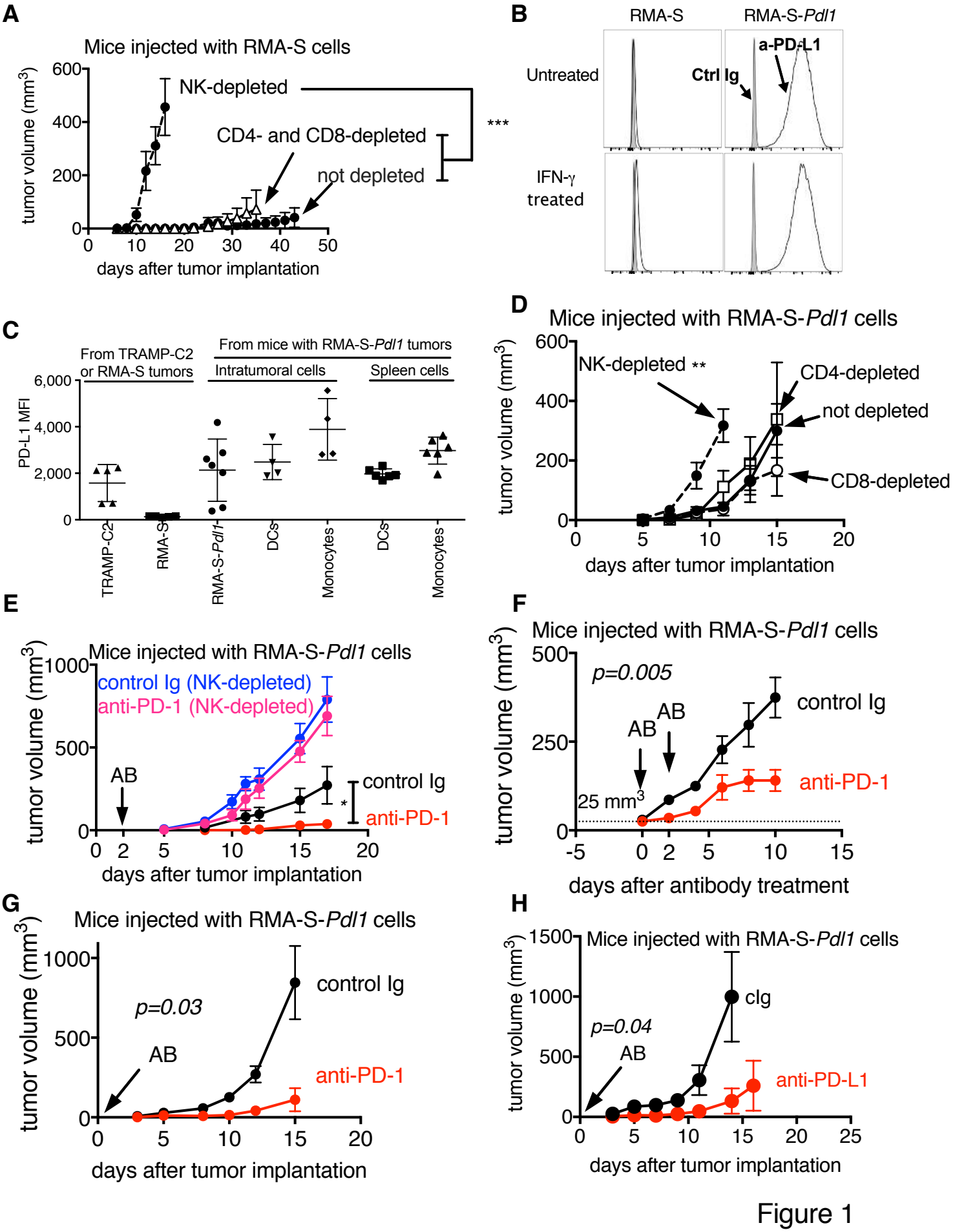
A
Mice injected with RMA-S cells
tumor volume (mm3)
600
400
200
0
NK-depleted
CD4- and CD8-depleted
not depleted
***
0
10
20
30
40
50
days after tumor implantation
B
RMA-S
RMA-S-Pdl1
Untreated
Ctrl Ig
a-PD-L1
IFN-γ treated
C
From TRAMP-C2 or RMA-S tumors
From mice with RMA-S-Pdl1 tumors
Intratumoral cells
Spleen cells
PD-L1 MFI
6,000
4,000
2,000
0
TRAMP-C2
RMA-S
RMA-S-Pdl1
DCs
Monocytes
DCs
Monocytes
D
Mice injected with RMA-S-Pdl1 cells
tumor volume (mm3)
600
400
200
0
NK-depleted **
CD4-depleted
not depleted
CD8-depleted
0
5
10
15
20
days after tumor implantation
E
Mice injected with RMA-S-Pdl1 cells
tumor volume (mm3)
1000
500
0
control Ig (NK-depleted)
anti-PD-1 (NK-depleted)
AB
*
control Ig
anti-PD-1
0
2
5
10
15
20
days after tumor implantation
F
Mice injected with RMA-S-Pdl1 cells
tumor volume (mm3)
500
250
0
p=0.005
AB
AB
control Ig
anti-PD-1
25 mm3
-5
0
2
5
10
15
days after antibody treatment
G
Mice injected with RMA-S-Pdl1 cells
tumor volume (mm3)
1000
500
0
p=0.03
AB
control Ig
anti-PD-1
0
5
10
15
20
days after tumor implantation
H
Mice injected with RMA-S-Pdl1 cells
tumor volume (mm3)
1500
1000
500
0
p=0.04
AB
clg
anti-PD-L1
0
5
10
15
20
25
days after tumor implantation

Figure 1

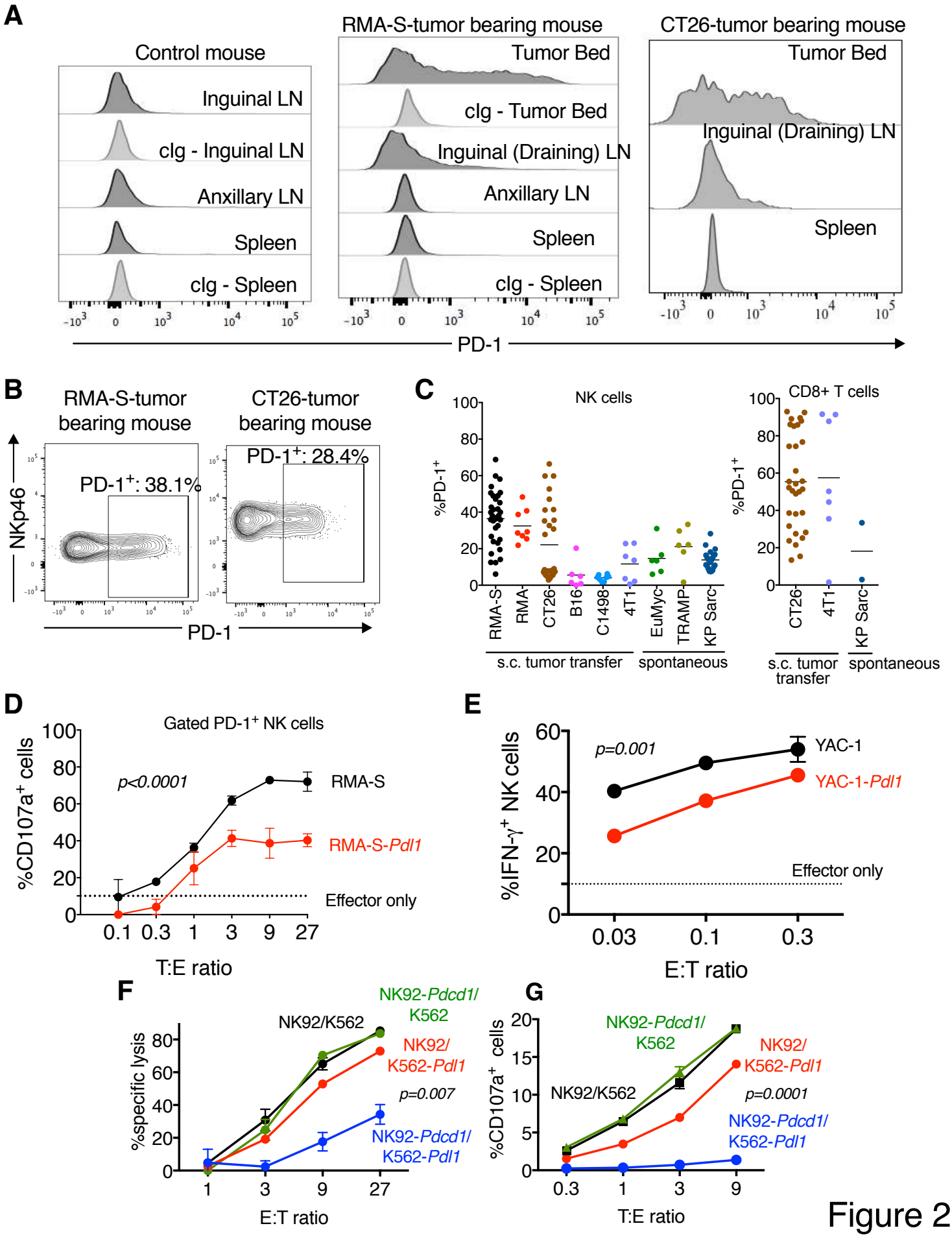
A
Control mouse
Inguinal LN
cIg - Inguinal LN
Anxillary LN
Spleen
cIg - Spleen
RMA-S-tumor bearing mouse
Tumor Bed
cIg - Tumor Bed
Inguinal (Draining) LN
Anxillary LN
Spleen
cIg - Spleen
CT26-tumor bearing mouse
Tumor Bed
Inguinal (Draining) LN
Spleen
PD-1
B
RMA-S-tumor bearing mouse
CT26-tumor bearing mouse
PD-1+: 38.1%
PD-1+: 28.4%
NKp46
PD-1
C
NK cells
CD8+ T cells
%PD-1+
RMA-S
RMA
CT26
B16
C1498
4T1
EuMyc
TRAMP
KP Sarc
s.c. tumor transfer
spontaneous
D
Gated PD-1+ NK cells
%CD107a+ cells
p<0.0001
RMA-S
RMA-S-Pdl1
Effector only
T:E ratio
E
%IFN-γ+ NK cells
p=0.001
YAC-1
YAC-1-Pdl1
Effector only
E:T ratio
F
%specific lysis
NK92/K562
NK92-Pdcd1/ K562
NK92/ K562-Pdl1
p=0.007
NK92-Pdcd1/ K562-Pdl1
E:T ratio
G
%CD107a+ cells
NK92-Pdcd1/ K562
NK92/ K562-Pdl1
NK92/K562
p=0.0001
NK92-Pdcd1/ K562-Pdl1
T:E ratio

Figure 2

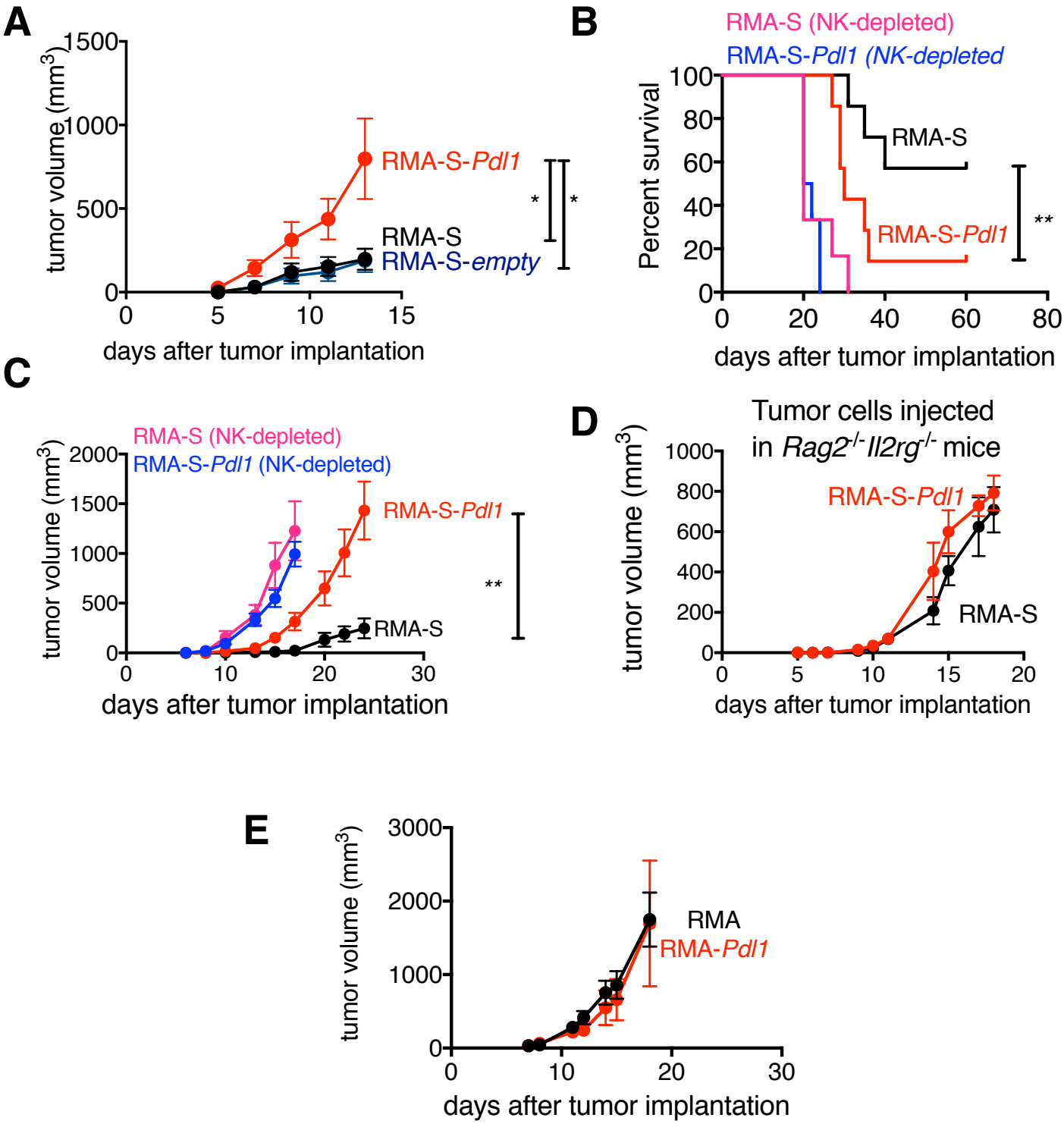
A
tumor volume (mm3)
1500
1000
500
0
0
5
10
15
days after tumor implantation
RMA-S-Pdl1
RMA-S
RMA-S-empty
*
*
B
RMA-S (NK-depleted)
RMA-S-Pdl1 (NK-depleted
Percent survival
100
80
60
40
20
0
0
20
40
60
80
days after tumor implantation
RMA-S
RMA-S-Pdl1
**
C
RMA-S (NK-depleted)
RMA-S-Pdl1 (NK-depleted)
tumor volume (mm3)
2000
1500
1000
500
0
0
10
20
30
days after tumor implantation
RMA-S-Pdl1
RMA-S
**
D
Tumor cells injected
in Rag2-/- Il2rg-/- mice
tumor volume (mm3)
1000
800
600
400
200
0
0
5
10
15
20
days after tumor implantation
RMA-S-Pdl1
RMA-S
E
tumor volume (mm3)
3000
2000
1000
0
0
10
20
30
days after tumor implantation
RMA
RMA-Pdl1

Figure 3

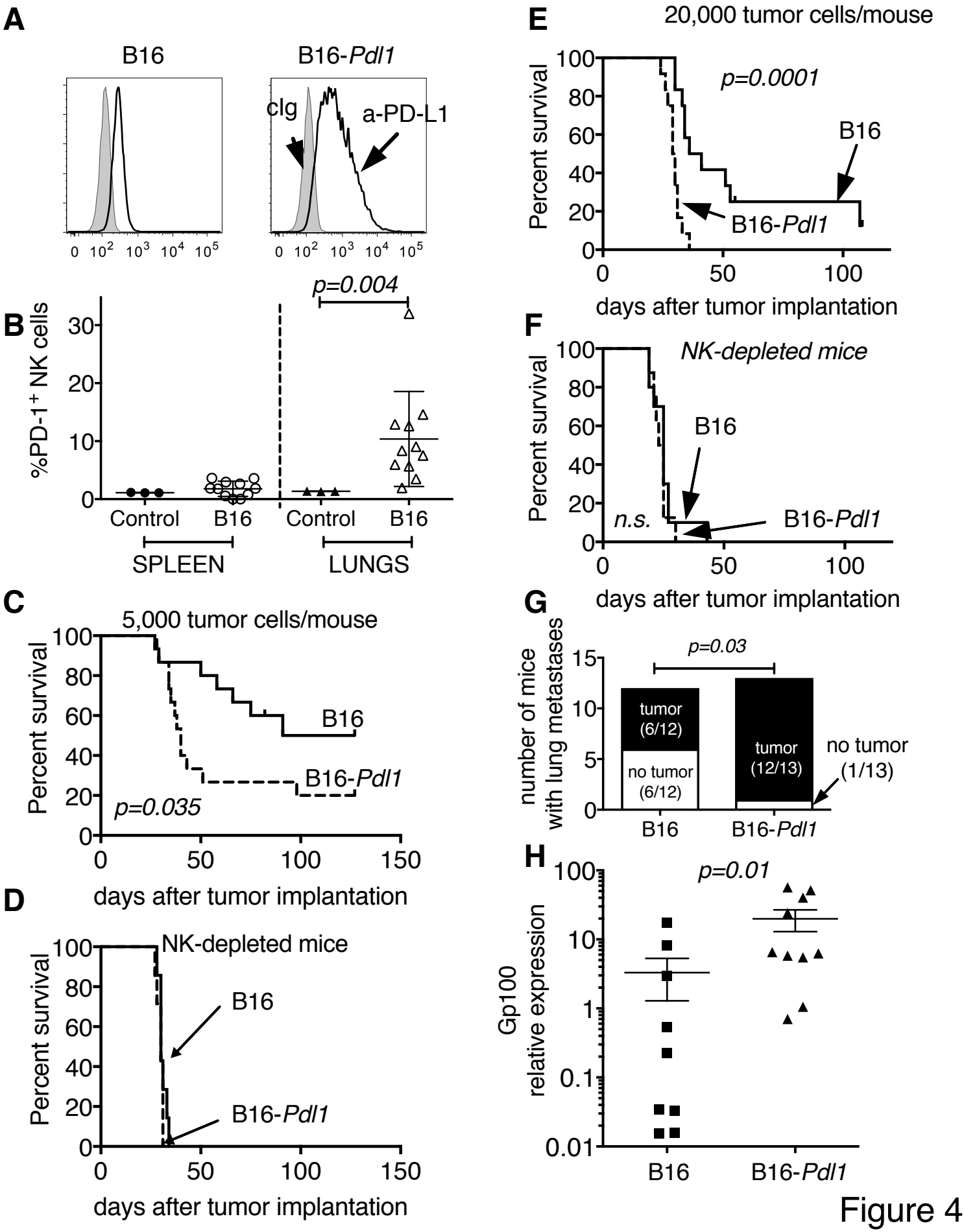
A
B16
B16-Pdl1
clg
a-PD-L1
0 10^2 10^3 10^4 10^5
B
p=0.004
%PD-1+ NK cells
Control
B16
Control
B16
SPLEEN
LUNGS
C
5,000 tumor cells/mouse
Percent survival
B16
B16-Pdl1
p=0.035
days after tumor implantation
D
NK-depleted mice
Percent survival
B16
B16-Pdl1
days after tumor implantation
E
20,000 tumor cells/mouse
Percent survival
p=0.0001
B16
B16-Pdl1
days after tumor implantation
F
NK-depleted mice
Percent survival
B16
n.s.
B16-Pdl1
days after tumor implantation
G
p=0.03
number of mice with lung metastases
tumor (6/12)
no tumor (6/12)
tumor (12/13)
no tumor (1/13)
B16
B16-Pdl1
H
p=0.01
Gp100 relative expression
B16
B16-Pdl1

Figure 4

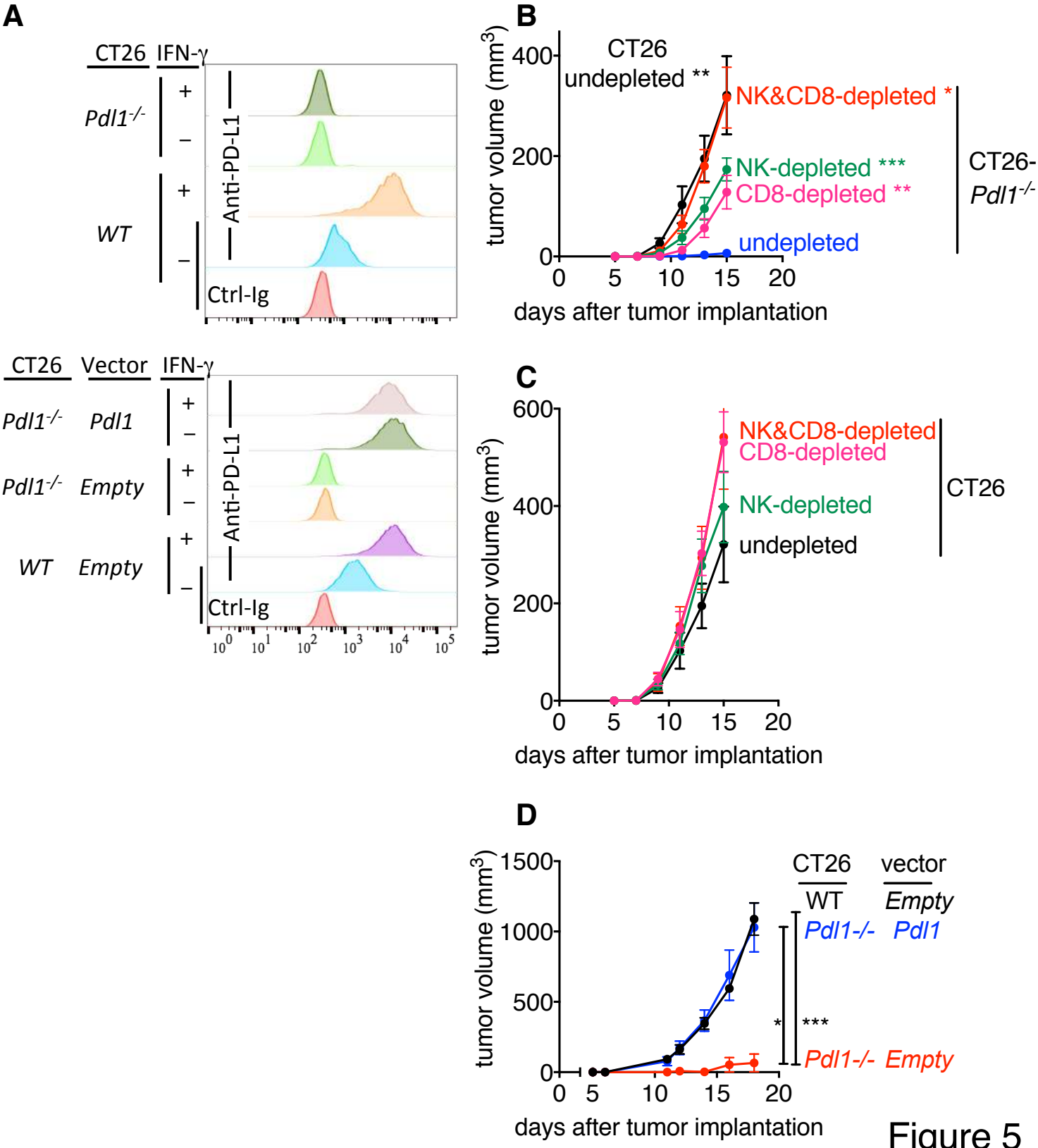
A
CT26 IFN-γ
Pdl1-/-
WT
+
–
Anti-PD-L1
Ctrl-Ig
CT26 Vector IFN-γ
Pdl1-/- Pdl1
Pdl1-/- Empty
WT Empty
B
CT26
undepleted **
NK&CD8-depleted *
NK-depleted ***
CD8-depleted **
undepleted
CT26-Pdl1-/-
tumor volume (mm3)
days after tumor implantation
C
NK&CD8-depleted
CD8-depleted
NK-depleted
undepleted
CT26
D
CT26 vector
WT Empty
Pdl1-/- Pdl1
Pdl1-/- Empty
*
***

Figure 5

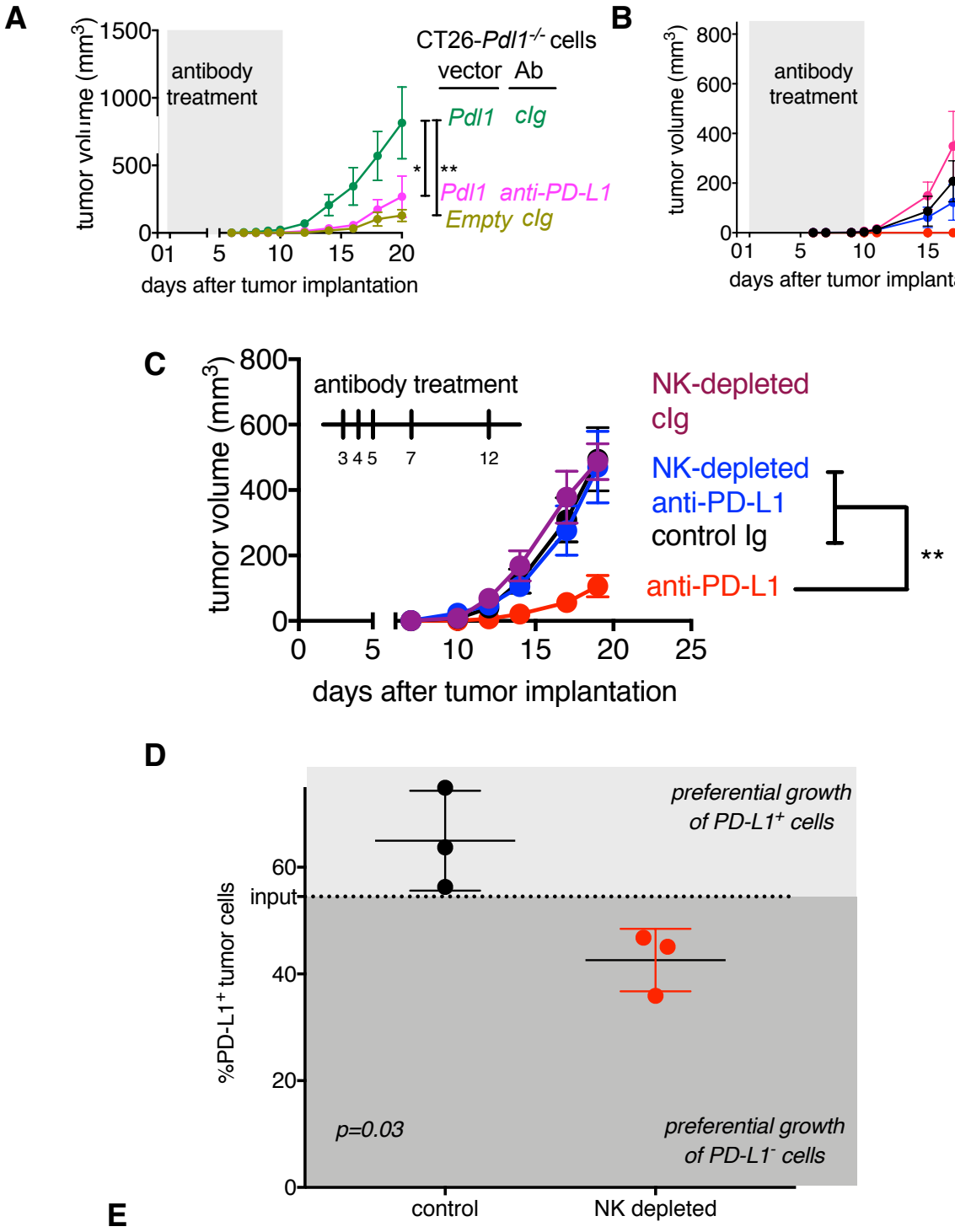
A
tumor volume (mm3)
1500
1000
500
0
antibody treatment
CT26-Pdl1-/- cells
vector Ab
Pdl1 clg
Pdl1 anti-PD-L1
Empty clg
*
**
01 5 10 15 20
days after tumor implantation
B
tumor volume (mm3)
800
600
400
200
0
antibody treatment
CD8-depleted anti-PD-L1*
control Ig*
NK-depleted anti-PD-L1*
anti-PD-L1
01 5 10 15 20
days after tumor implantation
C
tumor volume (mm3)
800
600
400
200
0
antibody treatment
3 4 5 7 12
NK-depleted clg
NK-depleted anti-PD-L1
control Ig
anti-PD-L1
**
0 5 10 15 20 25
days after tumor implantation
D
%PD-L1+ tumor cells
60
input
40
20
0
preferential growth of PD-L1+ cells
p=0.03
preferential growth of PD-L1- cells
control
NK depleted
E
%GrzB+ NK cells
80
60
40
20
0
*
*
CT26-Pdl1-/- +clg
CT26 +clg
CT26 +anti-PD-L1
CT26-Pdl1-/- +clg
CT26 +clg
CT26 +anti-PD-L1
gated PD-1+ NK cells
gated PD-1- NK cells

Figure 6

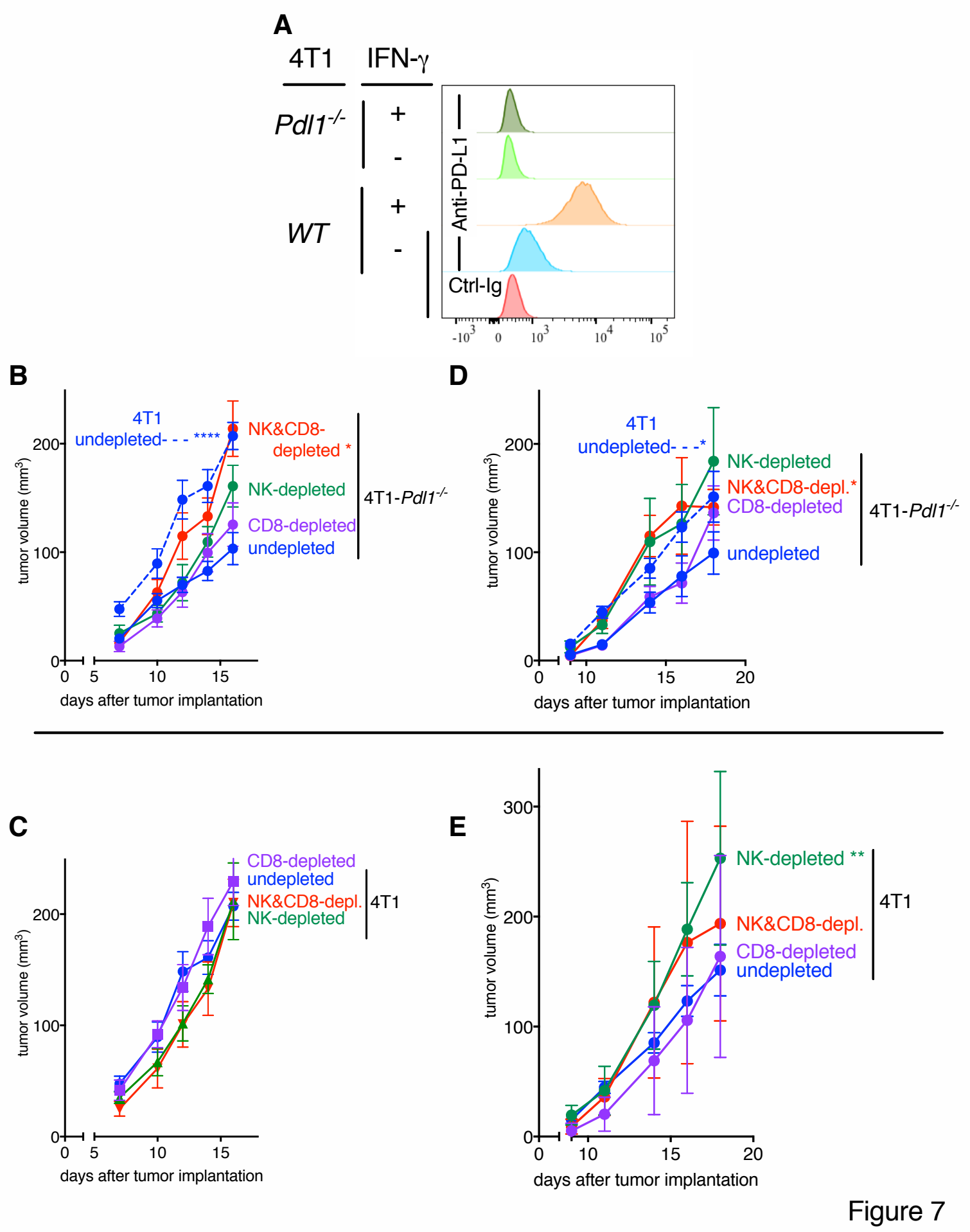
A
4T1
IFN-γ
Pdl1-/-
+
-
WT
+
-
Anti-PD-L1
Ctrl-Ig
-10^3
0
10^3
10^4
10^5
B
4T1
undepleted- - - ****
NK&CD8-depleted *
NK-depleted
CD8-depleted
undepleted
4T1-Pdl1-/-
tumor volume (mm3)
days after tumor implantation
D
4T1
undepleted- - -*
NK-depleted
NK&CD8-depl.*
CD8-depleted
undepleted
4T1-Pdl1-/-
tumor volume (mm3)
days after tumor implantation
C
CD8-depleted
undepleted
NK&CD8-depl.
NK-depleted
4T1
tumor volume (mm3)
days after tumor implantation
E
NK-depleted **
NK&CD8-depl.
CD8-depleted
undepleted
4T1
tumor volume (mm3)
days after tumor implantation

Figure 7

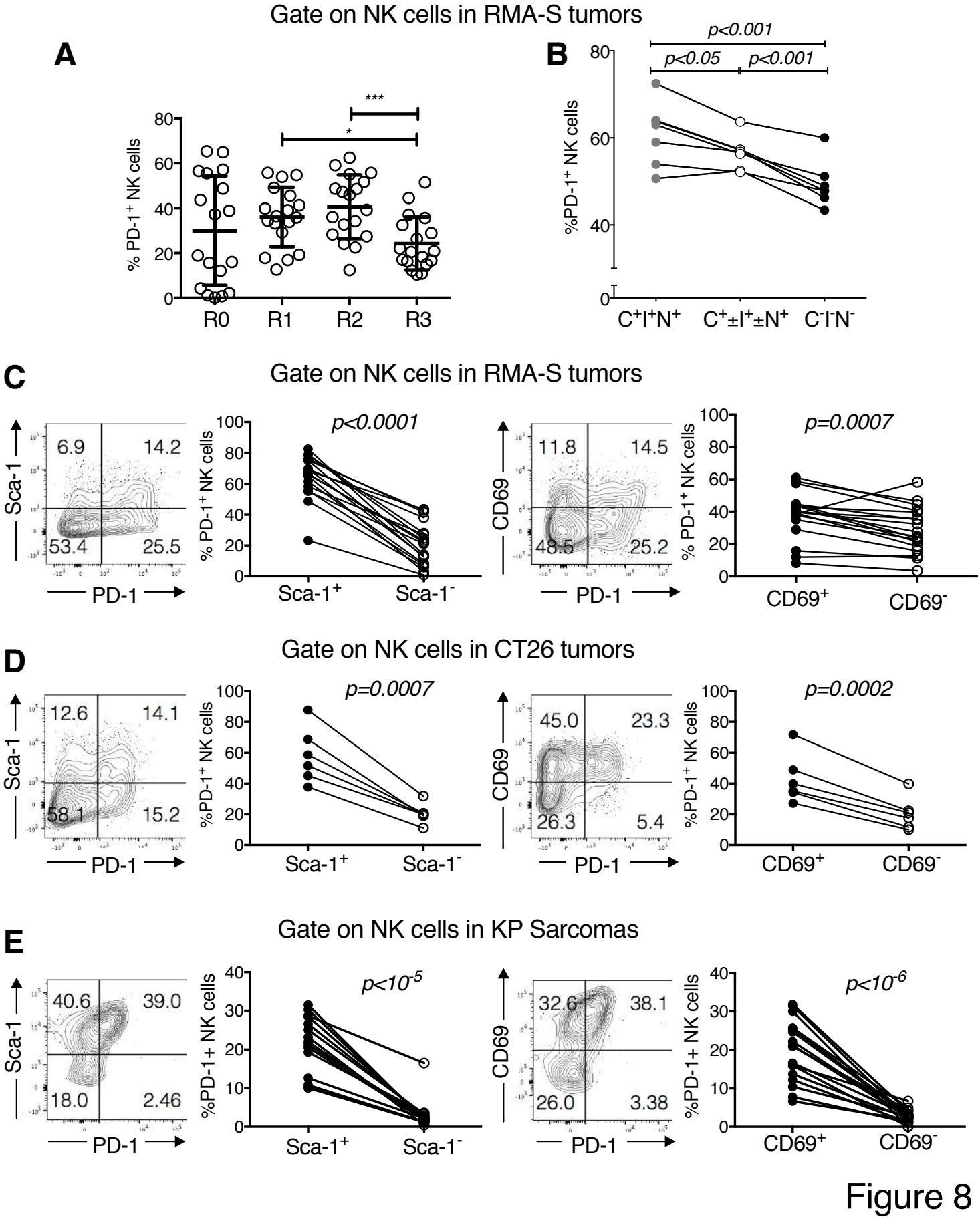
Gate on NK cells in RMA-S tumors
A
% PD-1+ NK cells
R0
R1
R2
R3
***
*
B
p<0.001
p<0.05
p<0.001
%PD-1+ NK cells
C+I+N+
C+±I+±N+
C-I-N-
C
Gate on NK cells in RMA-S tumors
Sca-1
PD-1
6.9
14.2
53.4
25.5
p<0.0001
Sca-1+
Sca-1-
CD69
11.8
14.5
48.5
25.2
p=0.0007
CD69+
CD69-
D
Gate on NK cells in CT26 tumors
12.6
14.1
58.1
15.2
p=0.0007
45.0
23.3
26.3
5.4
p=0.0002
E
Gate on NK cells in KP Sarcomas
40.6
39.0
18.0
2.46
p<10-5
32.6
38.1
26.0
3.38
p<10-6

Figure 8

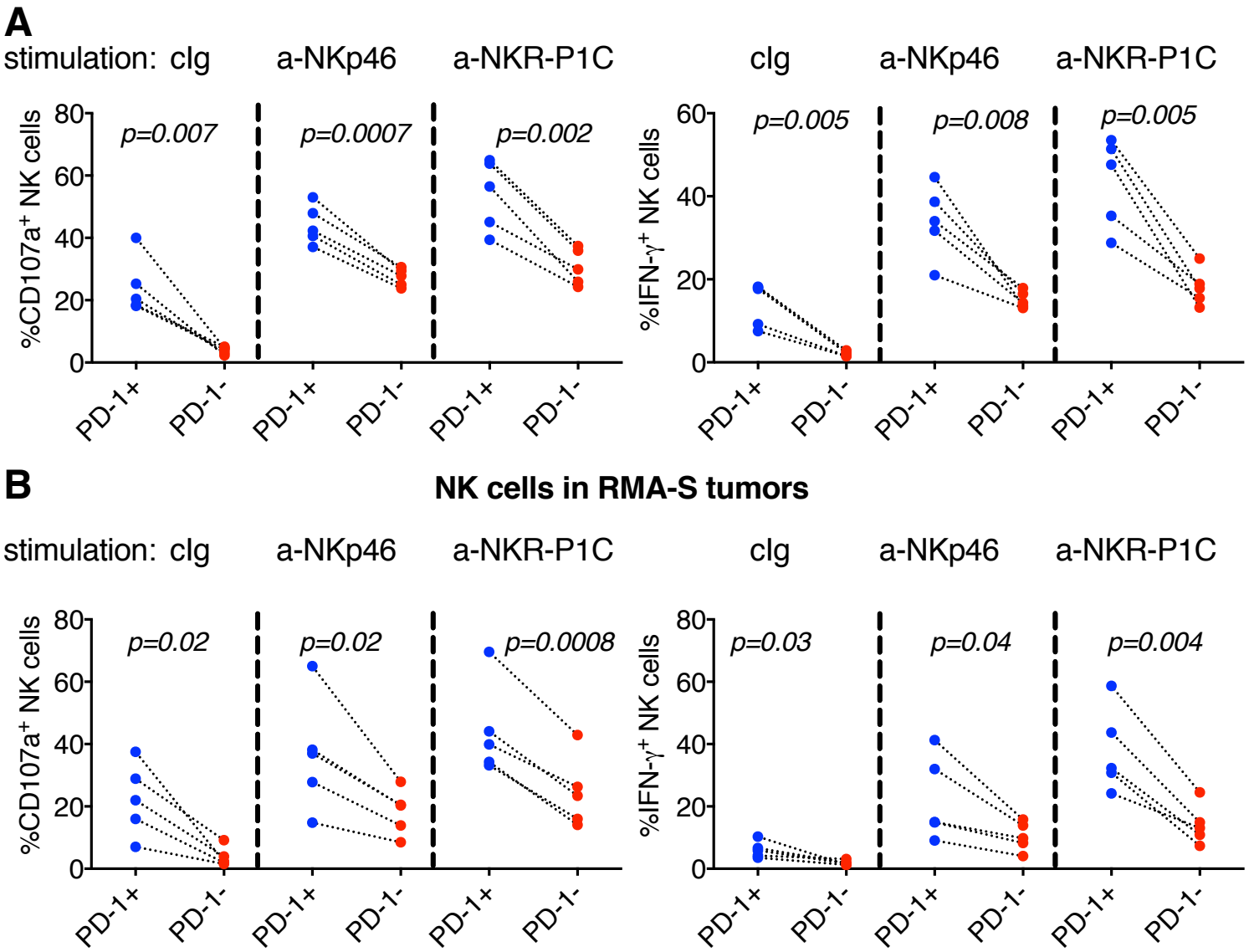
NK cells in RMA-S-Pdl1 tumors
A
stimulation: cIg
a-NKp46
a-NKR-P1C
%CD107a+ NK cells
p=0.007
p=0.0007
p=0.002
%IFN-γ+ NK cells
p=0.005
p=0.008
p=0.005
PD-1+
PD-1-
B
NK cells in RMA-S tumors
p=0.02
p=0.02
p=0.0008
p=0.03
p=0.04
p=0.004

Figure 9

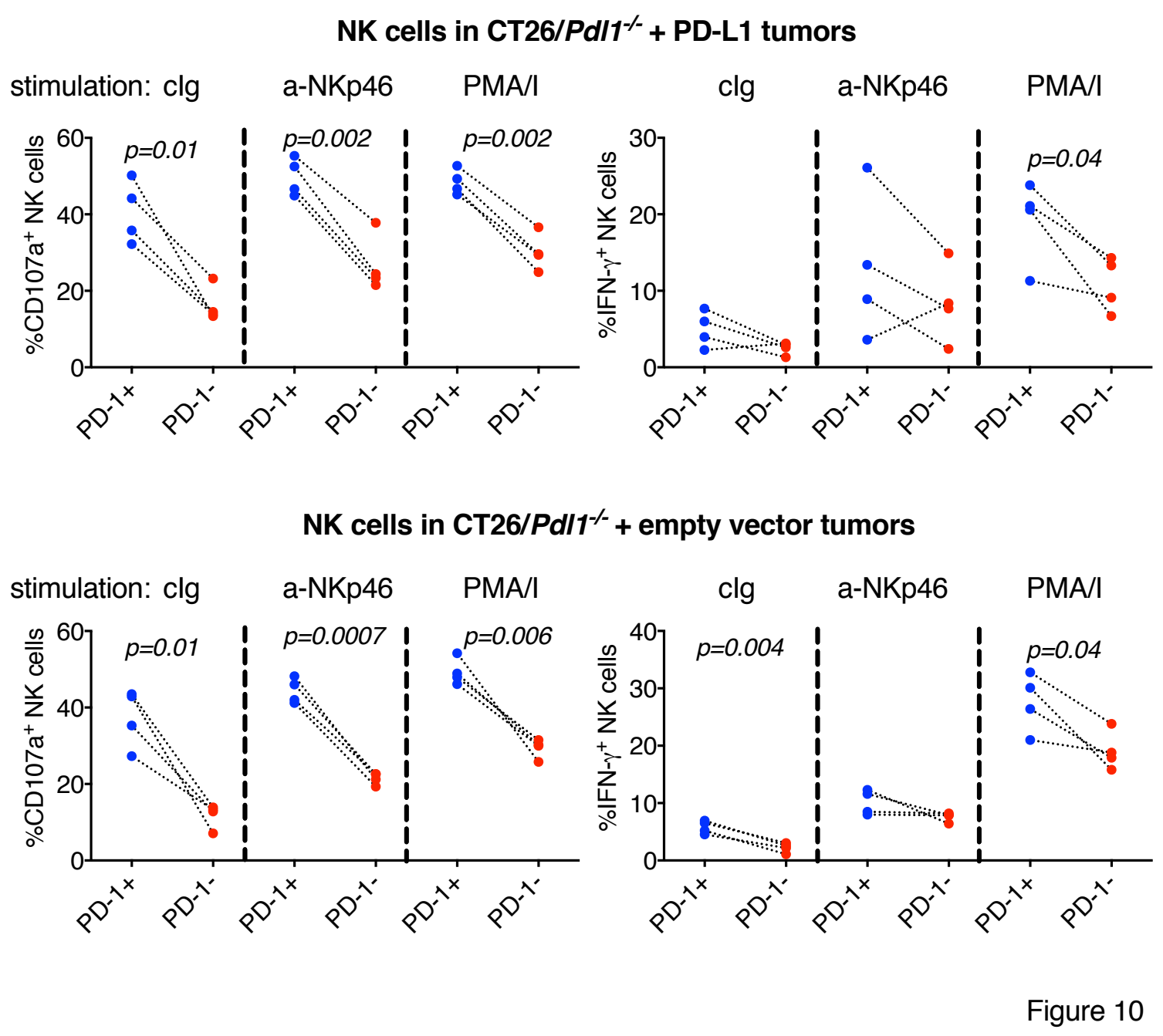
NK cells in CT26/Pdl1-/- + PD-L1 tumors
stimulation: clg
a-NKp46
PMA/I
%CD107a+ NK cells
p=0.01
p=0.002
p=0.002
%IFN-γ+ NK cells
p=0.04
PD-1+
PD-1-
NK cells in CT26/Pdl1-/- + empty vector tumors
p=0.01
p=0.0007
p=0.006
p=0.004
p=0.04

Figure 10

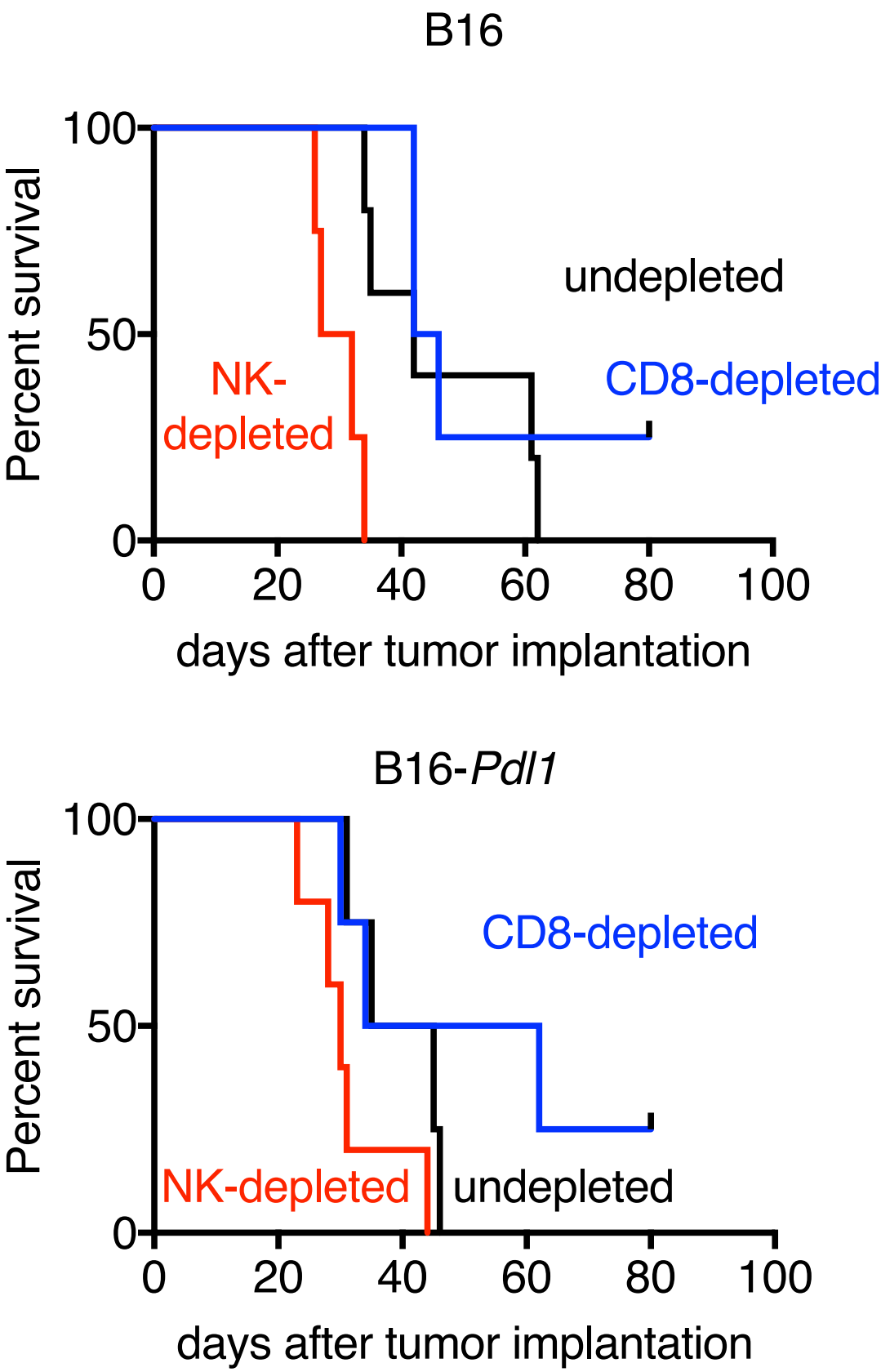

Supplementary Figure 1

CT26

4T1

RMA-S

B16

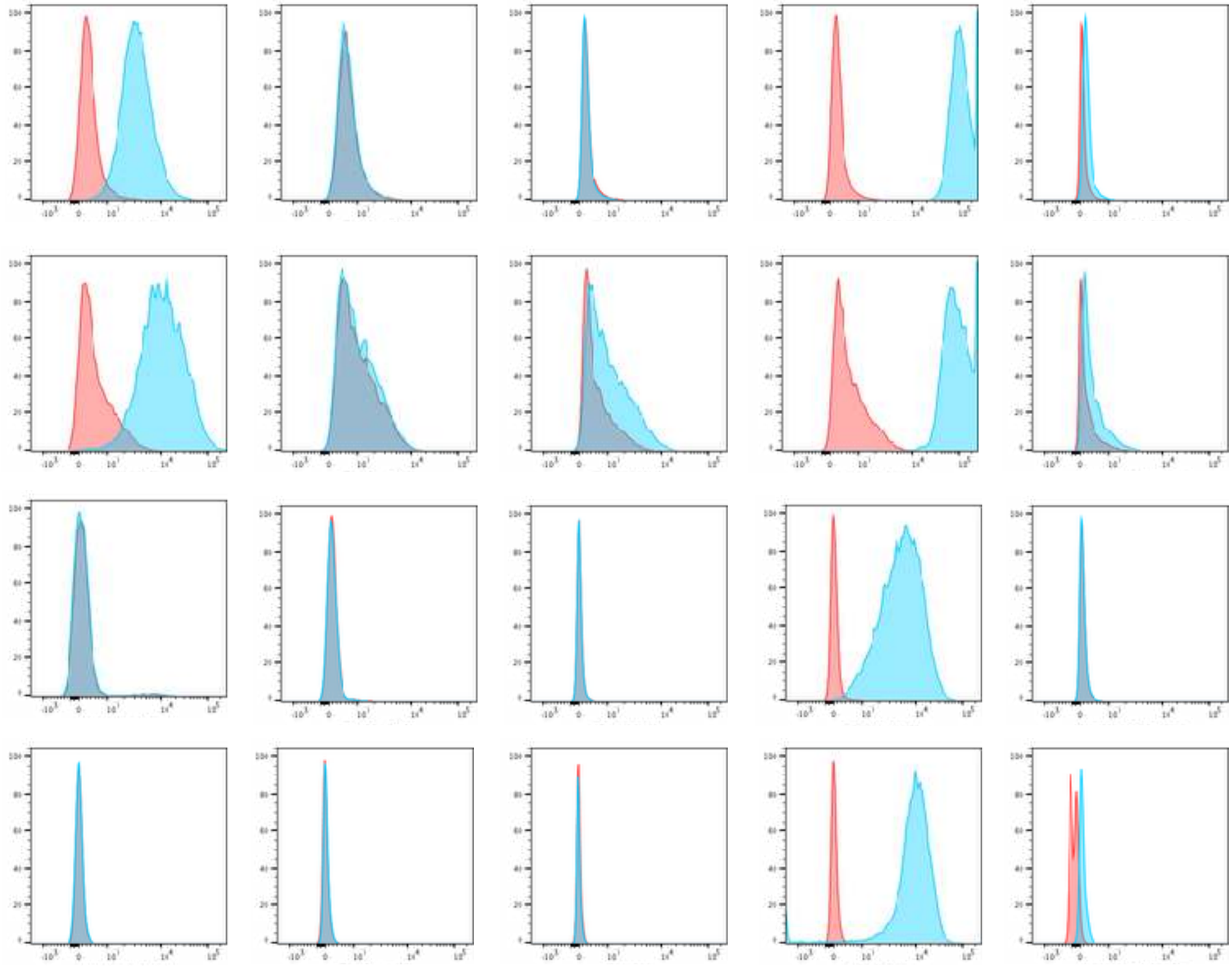

H60 Mult1 Rae1 PVR Nectin-2

Supplementary Figure 2

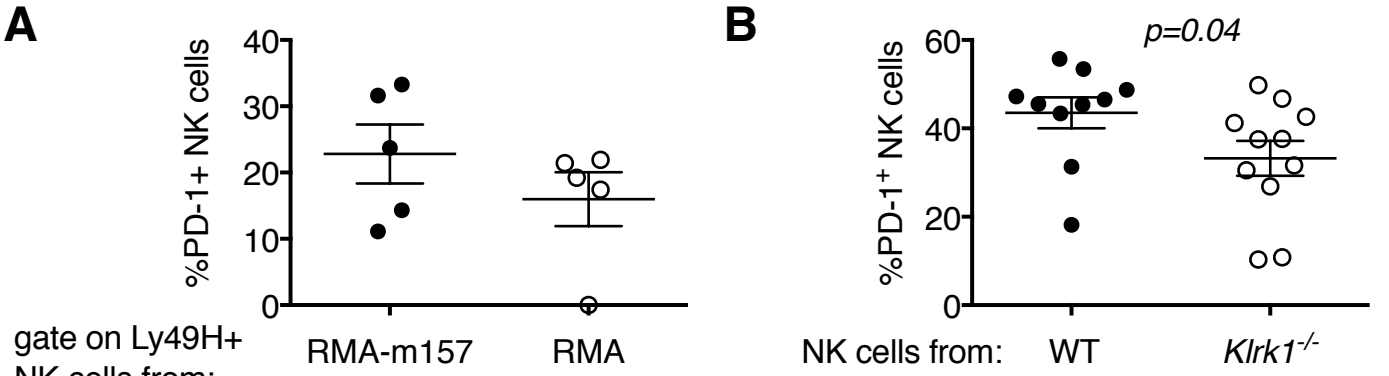

Supplementary Figure 3